A durable protective immune response to wild-type measles virus infection of macaques is due to viral replication and spread in lymphoid tissues

Wen-Hsuan W. Lin[1,*], **Eileen Moran**[1,†], **Robert J. Adams**[2], **Robert E. Sievers**[3], **Debra Hauer**[1], **Steven Godin**[4], **Diane E. Griffin**[1,‡]

[1]Department of Molecular Microbiology and Immunology, Johns Hopkins Bloomberg School of Public Health, Baltimore, MD 21205, USA.

[2]Department of Molecular and Comparative Pathology, Johns Hopkins University School of Medicine, Baltimore, MD 21218, USA.

[3]Department of Chemistry, University of Colorado, Boulder, CO 80309, USA.

[4]BASi, Gaithersburg, MD 20878, USA.

Abstract

Infection with wild-type (WT) measles virus (MeV) is an important cause of childhood mortality that leads to lifelong protective immunity in survivors. WT MeV and the live-attenuated MeV used in the measles vaccine (LAMV) are antigenically similar, but the determinants of attenuation are unknown, and protective immunity induced by LAMV is less robust than that induced by WT MeV. To identify factors that contribute to these differences, we compared virologic and immunologic responses after respiratory infection of rhesus macaques with WT MeV or LAMV. In infected macaques, WT MeV replicated efficiently in B and T lymphocytes with spreading throughout lymphoid tissues resulting in prolonged persistence of viral RNA. In contrast, LAMV replicated efficiently in the respiratory tract but displayed limited spread to lymphoid tissue or peripheral blood mononuclear cells. In vitro, WT MeV and LAMV replicated similarly in macaque primary respiratory epithelial cells and human lymphocytes, but LAMV-infected lymphocytes produced little virus. Plasma concentrations of interleukin-1β (IL-1β), IL-12, interferon-γ (IFN-γ), CCL2, CCL11, CXCL9, and CXCL11 increased in macaques after WT MeV but not LAMV infection. WT MeV infection induced more protective neutralizing,

hemagglutinin-specific antibodies and bone marrow plasma cells than did LAMV infection, although numbers of MeV-specific IFN-γ– and IL-4–producing T cells were comparable. Therefore, MeV attenuation may involve altered viral replication in lymphoid tissue that limited spread and decreased the host antibody response, suggesting a link between lifelong protective immunity and the ability of WT MeV, but not LAMV, to spread in lymphocytes.

INTRODUCTION

Elicitation of long-lived protective immunity is a major goal for the design and development of vaccines. It is therefore vital to understand the conditions under which lifelong protective immunity is established. Among viruses that cause acute infection in humans, wild-type (WT) measles virus (MeV) is remarkable for its ability to induce a sustained immune response and prolonged protection from reinfection (1–3). Lifelong protection from measles has been repeatedly observed and was first described by Panum (4) during an 1846 epidemic in the Faroe Islands.

MeV is a negative-strand enveloped RNA virus that encodes eight proteins: hemagglutinin (H) and fusion (F) surface glycoproteins, which mediate attachment and entry; the internal proteins nucleocapsid (N), matrix (M), phosphoprotein (P), and large polymerase (L), which control replication and virion production; and nonstructural proteins C and V encoded within the P reading frame that regulate the cellular response to infection. H protein is responsible for attachment to one or more of the multiple cellular receptors and is the primary target for neutralizing antibody (5, 6). After respiratory transmission, WT MeV spreads to local lymph nodes and then systemically to many sites including other lymphoid organs, liver, skin, and lung (7, 8).

In response to WT MeV infection, long-lived immune responses to multiple viral proteins are induced. These responses include cytotoxic $CD8^+$ T cells; $CD4^+$ T cells with T helper 1 (T_H1), T_H2, and T_H17 cytokine profiles; and B cells producing high-avidity neutralizing antibodies (9–13). Protective immunity to measles is mediated mainly by neutralizing antibodies and, to a lesser extent, by T cell responses (14–16). However, the mechanisms by which WT MeV efficiently induces lifelong protection from reinfection remain largely unknown.

Empirically developed by adaptation of a WT isolate of MeV to growth in tissue culture (17), the live-attenuated MeV (LAMV) used in the measles vaccine has been an effective tool for prevention of measles (18). After vaccination, LAMV causes very mild disease symptoms and little viremia, consistent with a substantial decrease in virulence compared to WT MeV (19). Although antigenically similar, sequences of current vaccine strains compared to WT MeV strains reveal amino acid differences in most viral proteins (fig. S1) (20, 21). Changes common to all vaccine strains exist in P/V/C, M, and H proteins, but no one change or combination of changes has been identified as responsible for attenuation of the virus (22).

Despite the antigenic similarities and cross-protection between WT MeV and LAMV, the duration of protective immunity after measles vaccination is more variable and not as long-

lived as after WT MeV infection (2, 23–25). Infection with both WT MeV and LAMV induces activation of CD4^{+} and CD8^{+} T cells and the production of neutralizing antibodies (26, 27). Protection after WT MeV infection is maintained for decades even in areas where measles is no longer endemic (2, 3). However, vaccine-induced MeV-specific antibodies and CD4^{+} T cells decrease over time (23, 28, 29) and may become undetectable, with secondary vaccine failure rates of about 5% 10 to 15 years after immunization (30, 31). Because of, in part, the difficulty of studying natural MeV infection in humans and a lack of small animal models, the biological basis of LAMV attenuation and the causes of less durable vaccine-induced immune responses remain unclear.

We hypothesized that the quality and longevity of protective immune responses are determined by the acute phase of MeV infection. To identify contributors to a robust and sustained protective immune response, we compared the virologic and immunologic consequences of primary infection with WT MeV or LAMV in a highly relevant rhesus macaque model (32–35). Because aerosol delivery of an LAMV vaccine is currently in clinical trials and to avoid differences due to route of infection, we compared macaques that were infected through the respiratory route with either the Edmonston-Zagreb (EZ) strain of LAMV or the Bilthoven strain of WT MeV. Our results demonstrated that efficient WT MeV production by lymphocytes followed by hematogenous spread throughout the lymphoid system and viral RNA persistence were associated with better induction of long-term protective immune responses compared to LAMV infection.

RESULTS

In vivo replication and tropism of WT MeV and LAMV after infection of macaques

Macaques infected by the respiratory route with WT MeV all developed skin rashes about 11 days after infection that resolved in 4 to 5 days. No animal infected with LAMV developed a rash. As an indicator of the extent of viral infection and spread, we analyzed the expression of MeV RNA in the respiratory tract (Fig. 1, A and B), peripheral blood mononuclear cells (PBMCs) (Fig. 1C), and draining mediastinal lymph nodes (Fig. 1D) of infected macaques using a reverse transcriptase polymerase chain reaction (RT-PCR) assay for the MeV N gene. Analysis of respiratory tract samples showed that seven of eight monkeys infected with WT MeV had detectable MeV RNA in nasal secretions between 7 and 14 days after infection (Fig. 1A). MeV RNA was present in lung tissue or bronchoalveolar lavage (BAL) fluid of all monkeys 7 days after infection with LAMV (Fig. 1B).

All WT MeV–infected macaques had cell-associated MeV RNA detectable in PBMCs 7, 14, and 21 to 24 days after infection (Fig. 1C) with the highest amount at day 7. Continued detection of MeV RNA in PBMCs up to 10 weeks after infection (34) when infectious virus was no longer recoverable was consistent with the previously observed slow clearance of viral RNA over 3 to 4 months in children with WT MeV infection (36, 37). Only 3 of 12 macaques in the LAMV-infected group had detectable MeV RNA in PBMCs at any time, principally at 21 to 24 days after infection ($P < 0.001$) (Fig. 1C). At 7 days after infection, only five LAMV-infected macaques had detectable MeV RNA in the draining lymph nodes (Fig. 1D), consistent with the lack of viral RNA in PBMCs.

After WT MeV infection, lymphocyte counts in the peripheral blood of macaques decreased with an increase after resolution of the rash at day 14, whereas infection of macaques with LAMV resulted in little change in lymphocyte counts over 28 days (Fig. 1, E and F). Respiratory infection of macaques with WT MeV led to efficient hematogenous spread and transient lymphopenia, whereas infection with LAMV led primarily to localized infection in the respiratory tract. The poor recovery of MeV RNA from the blood and secondary lymphoid tissues after LAMV infection suggested that vaccine virus attenuation selectively hindered virus replication in immune cells.

Identification of PBMCs infected with WT MeV

To identify the circulating PBMCs infected with WT MeV, we analyzed cells expressing MeV N protein by flow cytometry during the peak viremia at 7 and 10 days after infection (Fig. 2). Both $CD20^+$ B cells and $CD3^+$ T cells from WT MeV–infected macaques expressed the N protein (Fig. 2A), whereas cells from uninfected macaques did not (Fig. 2B). A higher percentage of B cells than T cells was infected at both time points (Fig. 2C). To determine whether certain subsets of T cells were preferentially infected, we further characterized $CD3^+$ T cells for expression of CD4, CD8, the MeV receptor CD150, and T cell memory markers CD28 and CD95 (Fig. 3A) (38). A higher proportion of $CD4^+$ than $CD8^+$ T cells were positive for MeV N protein, and the majority of both T cell subsets was central memory cells consistent with expression of CD150 by this cell population (Fig. 3B).

LAMV replication is restricted in lymphocytes but not respiratory epithelial cells

To further investigate mechanisms that affect in vivo viral spread, we used in vitro cultures to compare the ability of LAMV and WT MeV to produce infectious virus after infection of macaque primary differentiated respiratory epithelial cells and human PBMCs (Fig. 4). Cultures of macaque tracheal epithelial cells were infected with WT MeV or LAMV from both the apical and basal surfaces, and apical surface supernatant was analyzed for virus production. LAMV grew more rapidly and to a higher titer after both apical and basal infection than did WT MeV (Fig. 4A). Because WT MeV and LAMV have been reported to infect differentiated respiratory epithelial cells from the basal and not the apical surface (39, 40), we examined the apical surface supernatant by immunofluorescence microscopy to determine the source of infectious virus. Large numbers of viable MeV-infected multinucleated giant cells that had been shed from the epithelial surface of LAMV- and WT MeV–infected cultures were present in the supernatant (Fig. 4B).

To assess growth in immune cells, we infected PBMCs isolated from healthy human donors with WT MeV or LAMV at a high (2 to 5) (Fig. 4C) or low (0.5) (Fig. 4D) multiplicity of infection (MOI). Amounts of infectious MeV produced and released into culture supernatants at 40 to 48 hours after infection were measured by plaque formation in Vero cells expressing human SLAM (Vero/hSLAM) cells in vitro. Virus production was detected in the supernatants of all cultures infected with WT MeV but none of the cultures infected with LAMV (Fig. 4, C and D). LAMV production of infectious virus was impaired compared to WT MeV (MOI = 5) in both $CD4^+$ T cells (Fig. 4E) and $CD14^+$ myeloid cells (Fig. 4F).

To determine whether the decreased production of infectious virus was associated with less efficient viral entry of LAMV than WT MeV into lymphocytes, we stained CD4$^+$ T cells for intra-cellular expression of MeV N protein to identify by flow cytometry the percentage of cells infected at an MOI of 0.5 or 5.0 (Fig. 5A). More cells were positive for MeV N protein after LAMV infection (Fig. 5, B and D) than after WT MeV infection (Fig. 5, C and D). However, analysis of the amount of MeV N protein expressed by infected cells, as indicated by mean fluorescence inten-sity, revealed that more N protein was produced by WT MeV–infected cells (Fig. 5, A, C, and E) than LAMV-infected cells (Fig. 5, A, B, and E). Therefore, LAMV replication in lymphocytes was restricted at a step after viral entry, leading to inefficient production of infectious virus.

Cytokine and chemokine responses to LAMV or WT MeV infection of macaques

To compare the temporal development of immune responses induced by LAMV or WT MeV infection, we measured plasma concentrations of cytokines and chemokines indicative of innate and adaptive immune responses using a multiplex bead array (Fig. 6). There was early (day 3) induction of interleukin-12 (IL-12) and chemokines CCL2, CCL11, and CXCL11 and later (days 7 to 14) increases in CXCL9, IL-1β, and interferon-γ (IFN-γ) for macaques infected with WT MeV but not LAMV (Fig. 6). IL-17, β fibroblast growth factor (βFGF), CCL22, and macrophage inhibitory factor (MIF) were detectable but not significantly different ($P > 0.05$).

Antibody and long-lived plasma cell responses to macaque infection with LAMV or WT MeV

To compare MeV-specific adaptive immune responses to infection, we measured multiple aspects of the antibody response (Fig. 7). MeV infection induced amounts of MeV-specific binding immunoglobulin G (IgG) (Fig. 7A) and IgA (Fig. 7B) that were higher in the plasma of WT MeV–infected animals than LAMV-infected animals. Because antibody to the H protein is responsible for most of the neutralizing capacity in plasma (41), both H-specific binding antibody (Fig. 7C) and plaque reduction neutralizing activity (Fig. 7D) were measured. WT MeV induced more anti-H antibody and plaque reduction neutralizing antibody than did LAMV. Because maturation of antibody avidity is essential for neutralization of WT MeV and protective immunity (42), the avidity of MeV-specific IgG was also measured by enzyme immunoassay (EIA) (Fig. 7E). Avidities of antibody induced by WT MeV and LAMV were not different (Fig. 7E).

Circulating antibody is dependent on terminally differentiated long-lived plasma cells that reside primarily in bone marrow niches and continue to secrete antibody (43–46). To determine whether the numbers of plasma cells in bone marrow differed between groups, we assessed MeV-specific antibody-secreting cells about 1 year after infection (Fig. 7, F and G). More long-lived plasma cells were established in bone marrow after WT MeV infection than after LAMV infection. Furthermore, cells producing H-specific antibody were more abundant than those producing N-specific antibody in both groups (Fig. 7G).

T cell responses to LAMV or WT MeV infection of macaques

To determine whether induction of MeV-specific T cells in response to WT MeV or LAMV differed, we assessed PBMCs by enzyme-linked immunospot (ELISpot) assays for production of IFN-γ and IL-4 after stimulation with MeV and for H protein– and N protein– specific IFN-γ responses (Fig. 8). Numbers of N protein– and H protein–specific IFN-γ– producing spot-forming cells (SFCs) were similar for WT MeV– and LAMV-infected macaques both at 14 and 70 days after infection (Fig. 8A). Likewise, the numbers of MeV-specific IL-4–producing cells were also similar (Fig. 8B). To determine the time course of the appearance of MeV-specific IFN-γ–secreting lymphocytes in the circulation of infected macaques, we assessed IFN-γ–secreting cells over a 3- to 4-month period after infection (Fig. 8C). Similar temporal patterns were observed for WT MeV– and LAMV-infected macaques.

DISCUSSION

Respiratory infection of rhesus macaques with WT MeV and LAMV was characterized by distinct in vivo and in vitro virus replication profiles and immune responses. WT MeV replicated efficiently in B and T lymphocytes resulting in hematogenous virus spread, skin rash, and persistence of viral RNA. In contrast, after LAMV infection of macaques, the virus replicated well in the respiratory tract, but not in lymphoid cells, and showed limited spread. Innate immune responses differed, with induction of detectable amounts of cytokines IL-1β, IL-12, and IFN-γ and chemokines CCL2, CCL11, CXCL9, and CXCL11 in plasma after WT MeV infection but not after LAMV infection. Comparable numbers of MeV-specific T cells were induced by the two viruses, but higher amounts of protective antibody and more MeV-specific bone marrow–resident long-lived plasma cells developed after WT MeV infection compared to LAMV infection. Therefore, reduced virus replication in lymphoid tissue and hematogenous spread not only decreased the virulence of LAMV but also resulted in the development of a less robust protective antibody response. Thus, lifelong protective immunity after WT MeV infection may be associated with productive virus replication and spread in lymphoid tissue and slow clearance of viral RNA from these tissues.

WT MeV targets several types of cells during natural infection, e.g., B and T lymphocytes, monocytes and macrophages, dendritic cells, endothelial cells, and epithelial cells (Figs. 2 and 3) (8, 33, 47–51). However, there has been little analysis of the sites of LAMV replication, and the mechanism of attenuation has not been identified. In a recent study of intramuscular delivery of LAMV expressing enhanced green fluorescent protein (eGFP) to macaques, macrophages and dendritic cells were identified as the target cells in muscle (52).

Tropism of WT MeV compared to LAMV could reflect strain-specific differences in usage of the multiple host cellular receptors identified for MeV (53, 54). Membrane cofactor protein or CD46, a complement regulatory protein, is present on all nucleated cells but is used only by vaccine strains of MeV (55, 56). Poliovirus receptor–related 4 or nectin 4 is present on the basolateral surface of epithelial cells and is used by both WT and vaccine strains of MeV (57–59). Signaling lymphocytic activation molecule (SLAM) or CD150 is present on immature thymocytes, activated immune cells, and mature dendritic cells (60–62)

and is the most important receptor for infection of lymphoid tissue (63, 64) being used by both WT and vaccine MeV strains (65–74).

Therefore, one potentially important biologic difference between LAMV and WT MeV is the acquisition of efficient use of the CD46 receptor by vaccine strains (67, 68, 75). Tyrosine at position 481 of the H protein of vaccine strains (fig. S1) is a key determinant of the affinity of the viral H protein for CD46 (76, 77). WT MeV with asparagine at position 481 of the H protein interacts with SLAM, but not with CD46, and efficiently activates Toll-like receptor 2 (67, 69, 78). However, a mechanism by which gaining use of the CD46 receptor might lead to vaccine attenuation is not clear. Furthermore, evaluation in macaques of a recombinant chimeric MeV expressing vaccine or WT strain H protein indicated that attenuation involves an effect on virus replication rather than on receptor binding (79). This is consistent with our observations of equivalent infection of respiratory epithelial cells and lymphocytes by WT MeV and LAMV, but with differences in the amount of virus produced by immune cells (Figs. 4 and 5). Therefore, sequence differences in the H protein are unlikely to be the main determinants of virus attenuation.

Differences also exist in the sequences of the M protein between WT MeV and LAMV (fig. S1). The M dimer is crucial for recruitment of the virus nucleocapsid to the plasma membrane for virion assembly (80, 81); it promotes virion budding (82) and regulates viral RNA synthesis (83). Substitution of lysine for glutamine at position 89 is common to all MeV vaccine strains and enhances budding in Vero cells in vitro (84–86) but inhibits SLAM-dependent fusion and decreases virus growth in a B95a marmoset B cell line (87). Therefore, vaccine virus–associated sequence changes in M alter MeV replication, cell-cell fusion, and virion release in a cell type–dependent manner and may be an important determinant of attenuation.

Differential replication of WT MeV and vaccine strains of MeV has previously been studied in several relevant in vitro systems. Analysis of replication in primary human microvascular and umbilical vein endothelial cells demonstrated that vaccine strains of MeV infect endothelial cells more efficiently and replicate better than WT MeV (88, 89). LAMV replicates as well as WT MeV in monocyte-derived dendritic cells (90). Using eGFP-expressing recombinant viruses, nonepithelial SLAM-positive cells were identified as the main cells infected early in macaques by WT MeV, with later epithelial cell infection induced by infected lymphocytes (63, 91, 92). However, we show here that both WT MeV and vaccine strains can replicate in differentiated primary respiratory epithelial cells in vitro (Fig. 4, A and B). Respiratory infection of macaques by WT MeV leads to increasing amounts of virus in BAL fluid (93). We have shown that respiratory delivery of LAMV was associated with robust virus replication in the lung with only minimal viremia (Fig. 1) (94). These observations together indicate that respiratory epithelial cells are similarly susceptible to infection by WT MeV and LAMV in vivo as well as in vitro. Previous reports that polarized respiratory epithelial cells are not susceptible to MeV infection from the apical surface were based on a failure to detect eGFP-expressing cells in the intact monolayer after apical infection (39, 40). However, our results showed that virus was produced after apical infection (Fig. 4A). Shedding of infected respiratory epithelial cells (Fig. 4B) in vitro meant that they were no longer present in the monolayer, a response to infection observed with

respiratory syncytial virus (95). Therefore, virus attenuation may principally reflect the inability of LAMV to productively infect lymphoid tissue and cause viremia (Fig. 1) (35, 93).

Both B and T lymphocytes are infected during the viremia after WT MeV infection. A higher percentage of B cells than T cells are MeV positive, but T cells constitute a larger proportion of the circulating lymphocytes, so both types of cells are likely to be important for virus replication in lymphoid tissue and spread of infection. WT MeV and LAMV replication in primary lymphoid cells has been studied in human thymus organ cultures, tonsil explants, and isolated CD4$^+$ T cells (96–98). CD4$^+$CD8$^+$ double-positive thymocytes are susceptible to infection with LAMV and WT MeV, but vaccine strains replicate less efficiently and take longer to produce virus than do WT MeV strains (96). Although infection is initiated similarly in myeloid and lymphoid cells and use of CD46 facilitates infection of naïve lymphocytes, less infectious virus is produced by vaccine MeV than WT MeV (90, 92, 96, 97, 99, 100). Likewise, our data on infection of resting CD4$^+$ T cells, B cells, and monocytes from human peripheral blood showed that multiple types of immune cells displayed this defect in the production of LAMV (Figs. 4 and 5).

Our study showed that an important biologic consequence of limited LAMV replication in lymphoid tissue and systemic spread was a less vigorous induction of the immune response to MeV. This was evident in the differential stimulation of the systemic production of innate cytokines and chemokines early after infection with WT MeV or LAMV (Fig. 6). The C and V virus proteins regulate innate cellular responses to infection, and neither LAMV nor WT MeV induces type I IFN production in vitro or in vivo (90, 101). However, infection with WT MeV is associated with an increase in circulating concentrations of multiple cytokines and chemokines, including IL-1β, IFN-γ, CCL2, CCL11, and CCL22 in humans at the time of the skin rash (102, 103) and in macaques as early as 3 days after infection (Fig. 6). This has been little studied after LAMV infection in humans where small amounts of IFN-γ have been detected in sera (104). In our study, increases in these cytokines or chemokines were not detected in macaques after LAMV infection. These data are consistent with substantial activation of the inflammasome and nuclear factor κB signaling pathways of innate immune responses by WT MeV but not LAMV.

MeV infection induces both antibody and cellular immune responses, and neutralizing antibody is the best correlate of protection (16). Our previous studies in macaques have shown that neutralizing antibody predicts protection from disease (abrogation of skin rash) but not necessarily protection from infection. Our previous macaque studies also showed that T cells alone do not protect from either infection or disease but do facilitate clearance of viral RNA (15, 105–108). Although immune responses in our current study of WT MeV–infected and LAMV-infected macaques appeared to be qualitatively similar with respect to avidity and quantitatively similar with respect to T cell responses, the amounts of antibody in circulation, particularly of H-specific neutralizing antibody, were lower, and fewer H protein–specific long-lived plasma cells were established in the bone marrow after LAMV infection compared to WT MeV infection (Figs. 7 and 8). A less robust antibody response, but similar T cell response, suggests that restricted replication in lymphoid tissue led to more limited germinal center formation and production of antibody-secreting cells after LAMV

infection compared to WT MeV infection; even with limited replication in lymphoid tissue, virus replication in other tissues was sufficient to induce T cell responses. It is possible that robust antibody production is dependent on the observed persistence of viral RNA with prolonged expression of viral antigens in lymphoid tissue after infection with WT MeV (34). Differential induction of MeV-specific antibody and T cell responses was previously observed after LAMV delivery to the respiratory tract of macaques (15) where delivery to the upper respiratory tract induced MeV-specific IFN-γ–producing T cells but little anti-H antibody, whereas delivery to the lower respiratory tract (as in this study) induced neutralizing antibody and T cell responses.

The role of immunization route upon induction of protective immunity has not been systematically evaluated and is a limitation of this study. Early studies of LAMV using different routes of immunization showed poor antibody responses after nasal, conjunctival, or oral delivery in comparison to subcutaneous inoculation (109). A recent study of microneedle patch intradermal delivery has shown plaque reduction neutralization responses similar to subcutaneous delivery (110). Analysis of pulmonary immunization has generally shown it to be comparable to the subcutaneous route. Nebulized liquid LAMV induced lower antibody responses in young infants but similar responses in older children compared to subcutaneous immunization, and the dry powder formulation of LAMV induced antibody amounts comparable to those induced by subcutaneous inoculation in adults (111–114). However, none of these studies evaluated T cell responses.

Additional limitations to our study include the limited comparative evaluation of PBMCs and lymph nodes for T cell responses and antibody-secreting cells between WT MeV and LAMV. Previous studies in macaques of inhaled dry powder LAMV [estimated dose, 150 to 450 plaque-forming units (pfu)] showed better antibody and T cell responses than did subcutaneous delivery of 1000 pfu of LAMV (94, 115). WT MeV and LAMV replicated well in the respiratory tract (Fig. 1). Previous studies in macaques showed that infection proceeds similarly independent of dose (93), so differences observed in immune responses are unlikely to be due solely to differences in the infecting dose. However, the roles of both route of immunization and dose in determining the nature and specificity of immune responses to LAMV merit further study.

We hypothesized that lower amounts of antibody and shorter duration of the antibody response to LAMV compared to WT MeV infection in our study were due to limited virus replication in lymphoid tissue. This affected induction of follicular helper CD4$^+$ T cells and continued induction and germinal center selection of MeV-specific B cells necessary for the formation of long-lived affinity-matured plasma cells. The process by which lifelong immunity is established likely requires the prolonged presence of viral RNA and production of viral proteins in secondary lymphoid tissues after resolution of the acute phase of infection.

MATERIALS AND METHODS

Study design

This study was designed to compare in vitro and in vivo characteristics of infection of rhesus macaques (*Macaca mulatta*) with WT MeV or a vaccine strain of MeV. In vivo studies used respiratory infection of nonrandomized 2- to 3-year-old male and female macaques. Eight male macaques were infected with WT MeV (34). Seventeen male and 14 female macaques were infected by inhalation as part of studies evaluating aerosol delivery of LAMV as a dry powder (94, 111). Tissues were harvested at necropsy from 12 animals 7 days after LAMV infection; specimen collection from all other animals was by nasal swab, BAL, venipuncture, and bone marrow aspiration. These studies were complemented by in vitro infection of primary respiratory epithelial cells and lymphocytes from humans and macaques. Studies were not blinded, and no animals were excluded from analysis.

Thirty-five 2- to 3-year-old rhesus macaques negative for herpes B virus, tuberculosis, and antibody to MeV were obtained from Harlan Sprague Dawley (Indianapolis, IN) or the Johns Hopkins Primate Facility. Eight male macaques (15U, 46U, 55U, 67U, 40V, 43V, 55V, and 86U) were infected intratracheally with 10^4 tissue culture infectious dose 50% ($TCID_{50}$) of the Bilthoven strain of WT MeV (34). Seventeen male (264, 265, 270, 271, 273, 297 to 302, and 309 to 314) and 14 female (266, 275, 303 to 308, and 315 to 320) macaques were infected by inhalation of an aerosolized 10^5 pfu of a dry powder formulation of LAMV as part of efficacy and pre–phase 1 toxicology studies (94, 111). For the toxicology study, tissues were harvested at necropsy (lung, mediastinal lymph nodes, etc.) from 12 animals 7 days after infection. Respiratory specimens were collected by BAL; heparinized blood was collected from the femoral vein; and heparinized bone marrow was collected from the femur. All procedures were performed under ketamine anesthesia supplemented with halothane as needed and in accordance with protocols approved by the Avanza Laboratory or the Johns Hopkins Institutional Animal Care and Use Committees.

Viruses and cells

The Chicago-1 and EZ (Serum Institute of India) strains of LAMV were grown and assayed in Vero cells (American Type Culture Collection). EZ used for immunization was formulated as an inhalable dry powder as previously described (94). The Bilthoven strain of WT MeV (gift of A. Osterhaus, Erasmus University) was grown in phytohemagglutinin-stimulated human cord blood mononuclear cells and assayed by syncytium formation in B95–8 cells (116) or in Vero/hSLAM [gift of Y. Yanagi, Kyoto University; (74)]. Vero and Vero/hSLAM cells were grown in Dulbecco's modified Eagle's medium (DMEM) supplemented with 10% fetal bovine serum (FBS).

Human PBMCs from healthy adults were obtained from the Johns Hopkins Hospital Blood Bank and isolated by Percoll gradient centrifugation. $CD4^+$ T cells and $CD14^+$ myeloid cells were isolated from PBMCs with CD4 and CD14 microbeads according to the manufacturer's instructions (Miltenyi Biotec).

To establish cultures of primary respiratory epithelial cells, cells harvested with pronase from the tracheas of three uninfected rhesus macaques were depleted of fibroblasts by

differential adherence, expanded in basic medium (DMEM/F-12, 5% FBS, insulin, transferrin, cholera toxin, epidermal growth factor, and bovine pituitary extract) and frozen in aliquots as previously described (117). To establish differentiated tracheal epithelial cell cultures, cells were plated on collagen-coated Transwell inserts with 0.4-mm pore 0.33-cm^2 Transwell-Clear supported membranes (Corning Costar) at a density of 1×10^5 cells/cm^2. The cells were grown in liquid culture (basic medium + retinoic acid) until they reached a transepithelial resistance of >1000 ohm/cm^2. Transepithelial resistance was measured with the Millipore Millicell-ERS (Millipore). The cells were then differentiated at an air-liquid interface into pseudostratified epithelium that included both mucous-producing and ciliated cells.

RT-PCR analysis of MeV RNA

MeV RNA was detected and measured by RT-PCR for the N gene as previously described (34). Briefly, RNA was isolated, and the N gene was amplified from cells or tissues (Applied Biosystems Prism 7700) using TaqMan primers and probe. For nasal swab cell pellets, RT-PCR products were run on gels and read as positive or negative. For all other samples, copy number was determined by comparison to a standard curve constructed from 1 to 10^6 copies of RNA synthesized by in vitro transcription from a plasmid containing the Edmonston MeV N gene. The sensitivity of the assay was 10 copies. Data were normalized to the glyceraldehyde-3-phosphate dehydrogenase (GAPDH) control and expressed as (copies of MeV N RNA/ copies of GAPDH RNA) $\times$ 5000.

In vitro MeV infection and virus assay

Differentiated macaque tracheal epithelial cells from three individual macaques were infected for 4 hours at 37°C with WT MeV (Bilthoven) or LAMV (EZ) at an MOI of 4.5 through the apical surface in a total volume of 150 μl or basolateral surface in a total volume of 500 μl. The inoculum was removed, and cells were washed three times with phosphate-buffered saline containing Ca^{2+} and Mg^{2+}. Infectious MeV in the apical supernatant fluids was analyzed by cocultivation in duplicate of serially diluted supernatant fluids with Vero or Vero/ hSLAM cells. Cultures were scored for cytopathic effect after 5 days, and data were reported as TCID$_{50}$ per milliliter.

Immunocytochemistry

Cells shed into the apical supernatant fluids of tracheal epithelial cell cultures were plated on 96-well flat-bottom plates and centrifuged, and supernatant fluid was removed. The cells were then fixed and permeablized using the BD Cytofix/Cytoperm kit. After washing, the cells were incubated with fluorescein isothiocyanate (FITC)–conjugated MeV N-specific antibody (Chemicon/MilliporeSigma) in cytoperm wash solution for 1 hour at 4°C, washed, and incubated with $4'$,6-diamidino-2-phenylindole (DAPI) for 15 min. The cells were observed using a Nikon inverted TE200 microscope.

Flow cytometry

A total of 10^6 fresh PBMCs were stained with ViViD LIVE/DEAD discriminator (Invitrogen) and antibodies to CD3, CD4, CD8, CD14, CD28, CD95, CD150 (BD

Biosciences), and CD20 (eBioscience). Cells were permeabilized using the BD Cytofix/ Cytoperm kit and stained with FITC-conjugated antibody to MeV N. Cells were read on a BD LSR II or FACSCanto II flow cytometer. A total of 400,000 events were collected per sample. Analysis was performed using FlowJo software (version 8.8.6; FlowJo Inc.).

Cytokine and chemokine assays

Levels of cytokines and chemokines in plasma were determined using a Luminex 28-plex monkey cytokine/chemokine panel (Invitrogen) on samples from five WT MeV–infected monkeys (46U, 55U, 67U, 40V, and 43V) and five LAMV-infected monkeys (264, 266, 313, 318, and 319). The panel included IFN-γ, IL-1β, IL-1RA, IL-2, IL-4, IL-5, IL-6, IL-10, IL-12, IL-15, IL-17, CCL2, CCL3, CCL4, CCL5, CCL11, CCL22, CXCL8, CXCL9, CXCL11, MIF, βFGF, HGF (hepatocyte growth factor), GCSF (granulocyte colony-stimulating factor), and GMCSF (granulocyte-macrophage colony-stimulating factor). Levels of rhesus IFNα2 (PBL Assay Science) and IFNβ (LifeSpan Biosciences) were determined by EIAs according to the manufacturers' instructions. Several cytokines were not (IFNα2, IL-4, IL-5, IL-6, IL-10, IL-15, GCSF, and GMCSF) or were rarely (IFN, HGF, IL-1RA, CCL3, CCL4, and CXCL8) detected. Amounts of CXCL5 were high in all samples due to platelet contamination.

Antibody assays

For PRN assays, the Chicago-1 strain of MeV was mixed with serially diluted plasma and assayed for plaque formation on Vero cells in triplicate. The dilution of plasma that resulted in 50% plaque reduction was calculated. MeV-specific IgG and IgA and H-specific IgG in plasma were measured by EIAs using MaxiSorp plates (Nunc) coated with lysates from MeV-infected Vero cells (1.16 µg of protein per well; Advanced Biotechnologies) or MeV H-expressing L cells (118) as previously described (15). Avidity of MeV-specific IgG was determined by adding increasing concentrations of ammonium thiocyanate (NH$_4$SCN; 0.5 to 3 M) to the EIA assay for 15 min. The avidity index was calculated as the concentration of NH$_4$SCN at which 50% of the bound antibody was eluted.

To measure antibody-secreting cells in the bone marrow, cells isolated from bone marrow aspirates by density gradient centrifugation using Lympholyte Mammal (Cedarlane Laboratories) were incubated for 6 hours with Multiscreen ELISpot plates (MilliporeSigma) coated with MeV-infected Vero cell lysate, H-expressing L cell lysate, or baculovirus-expressed N. Bound immunoglobulin was detected with horseradish peroxidase (HRP)–conjugated goat anti-monkey IgG (Nordic), developed with stable diaminobenzidine (DAB) solution and read on an ImmunoSpot plate reader (Cellular Technology).

T cell assays

ELISpot assays were used to measure IFN-γ– and IL-4–producing lymphocytes as previously described (34). Briefly, Multiscreen ELISpot plates were coated with antibody to human IFN-γ or IL-4 (BD Biosciences) and blocked with RPMI 1640/10% FBS, and 1×10^5 to 5×10^5 fresh PBMCs were added along with pooled MeV peptides (1 µg/ml; 20-mers overlapping by 11 amino acids) from the MeV H or N proteins, concanavalin A (5 µg/ml), or medium alone. After 40 hours of incubation, plates were developed with biotinylated

antibody to IFN-γ (Mabtech) or IL-4 (BD Biosciences), followed by HRP-conjugated avidin and DAB solution, and scanned. Data were analyzed using ImmunoSpot, version 3.0 software. Results are presented as the number of SFCs per 10^6 PBMCs.

Statistical analysis

For statistical analyses, we performed two-tailed Student's t test ($\alpha = 0.05$) or nonparametric analysis with Mann-Whitney U test to compare two groups, or analysis of variance (ANOVA) with Bonferroni post hoc tests for comparing multiple groups. All data were analyzed using GraphPad Prism software. Statistical significance was determined as *$P <$ 0.05, **$P <$ 0.01, and ***$P <$ 0.001.

Supplementary Material

Refer to Web version on PubMed Central for supplementary material.

Acknowledgments:

REFERENCES AND NOTES

1. Amanna IJ, Slifka MK, Mechanisms that determine plasma cell lifespan and the duration of humoral immunity. Immunol. Rev 236, 125–138 (2010). [PubMed: 20636813]

2. Chen CJ, Lee PI, Hsieh YC, Chen PY, Ho YH, Chang CJ, Liu DP, Chang FY, Chiu CH, Huang YC, Lee CY, Lin TY, Waning population immunity to measles in Taiwan. Vaccine 30, 6721–6727 (2012). [PubMed: 22634294]

3. Amanna IJ, Carlson NE, Slifka MK, Duration of humoral immunity to common viral and vaccine antigens. N. Engl. J. Med 357, 1903–1915 (2007). [PubMed: 17989383]

4. Panum P, Observations made during the epidemic of measles on the Faroe Islands in the year 1846. Med. Classics 3, 829–886 (1938).

5. Santiago C, Celma ML, Stehle T, Casasnovas JM, Structure of the measles virus hemagglutinin bound to the CD46 receptor. Nat. Struct. Mol. Biol 17, 124–129 (2010). [PubMed: 20010840]

6. Hashiguchi T, Ose T, Kubota M, Maita N, Kamishikiryo J, Maenaka K, Yanagi Y, Structure of the measles virus hemagglutinin bound to its cellular receptor SLAM. Nat. Struct. Mol. Biol 18, 135–141 (2011). [PubMed: 21217702]

7. Nozawa Y, Ono N, Abe M, Sakuma H, Wakasa H, An immunohistochemical study of Warthin-Finkeldey cells in measles. Pathol. Int 44, 442–447 (1994). [PubMed: 8055110]

8. Moench TR, Griffin DE, Obriecht CR, Vaisberg AJ, Johnson RT, Acute measles in patients with and without neurological involvement: Distribution of measles virus antigen and RNA. J. Infect. Dis 158, 433–442 (1988). [PubMed: 3042879]

9. van Binnendijk RS, Poelen MC, Kuijpers KC, Osterhaus AD, Uytdehaag FG, The predominance of CD8+ T cells after infection with measles virus suggests a role for CD8+ class I MHC-restricted cytotoxic T lymphocytes (CTL) in recovery from measles. Clonal analyses of human CD8+ class I MHC-restricted CTL. J. Immunol 144, 2394–2399 (1990). [PubMed: 2107259]

10. Mongkolsapaya J, Jaye A, Callan MF, Magnusen AF, McMichael AJ, Whittle HC, Antigen-specific expansion of cytotoxic T lymphocytes in acute measles virus infection. J. Virol 73, 67–71 (1999). [PubMed: 9847308]

11. El Mubarak HS, Ibrahim SA, Vos HW, Mukhtar MM, Mustafa OA, Wild TF, Osterhaus AD, de Swart RL, Measles virus protein-specific IgM, IgA, and IgG subclass responses during the acute and convalescent phase of infection. J. Med. Virol 72, 290–298 (2004). [PubMed: 14695672]

12. Nelson AN, Putnam N, Hauer D, Baxter VK, Adams RJ, Griffin DE, Evolution of T cell responses during measles virus infection and RNA clearance. Sci. Rep 7, 11474 (2017). [PubMed: 28904342]

13. Moss WJ, Ryon JJ, Monze M, Griffin DE, Differential regulation of interleukin (IL)-4, IL-5, and IL-10 during measles in Zambian children. J. Infect. Dis 186, 879–887 (2002). [PubMed: 12232827]

14. Samb B, Aaby P, Whittle HC, Seck AM, Rahman S, Bennett J, Markowitz L, Simondon F, Serologic status and measles attack rates among vaccinated and unvaccinated children in rural Senegal. Pediatr. Infect. Dis. J 14, 203–209 (1995). [PubMed: 7761185]

15. Lin WH, Pan CH, Adams RJ, Laube BL, Griffin DE, Vaccine-induced measles virus-specific T cells do not prevent infection or disease but facilitate subsequent clearance of viral RNA. MBio 5, e01047 (2014). [PubMed: 24736226]

16. Chen RT, Markowitz LE, Albrecht P, Stewart JA, Mofenson LM, Preblud SR, Orenstein WA, Measles antibody: Reevaluation of protective titers. J. Infect. Dis 162, 1036–1042 (1990). [PubMed: 2230231]

17. Katz SL, Enders JF, Holloway A, The development and evaluation of an attenuated measles virus vaccine. Am. J. Public Health Nations Health 52 (Suppl 2), 5–10 (1962). [PubMed: 14454407]

18. Bellini WJ, Rota PA, Biological feasibility of measles eradication. Virus Res. 162, 72–79 (2011). [PubMed: 21963661]

19. Lievano F, Galea SA, Thornton M, Wiedmann RT, Manoff SB, Tran TN, Amin MA, Seminack MM, Vagie KA, Dana A, Plotkin SA, Measles, mumps, and rubella virus vaccine (M-M-R™II): A review of 32 years of clinical and postmarketing experience. Vaccine 30, 6918–6926 (2012). [PubMed: 22959986]

20. Takeda M, Sakaguchi T, Li Y, Kobune F, Kato A, Nagai Y, The genome nucleotide sequence of a contemporary wild strain of measles virus and its comparison with the classical Edmonston strain genome. Virology 256, 340–350 (1999). [PubMed: 10191199]

21. Bankamp B, Takeda M, Zhang Y, Xu W, Rota PA, Genetic characterization of measles vaccine strains. J. Infect. Dis 204 (Suppl 1), S533–S548 (2011). [PubMed: 21666210]

22. Bankamp B, Hodge G, McChesney MB, Bellini WJ, Rota PA, Genetic changes that affect the virulence of measles virus in a rhesus macaque model. Virology 373, 39–50 (2008). [PubMed: 18155263]

23. Christenson B, Bottiger M, Measles antibody: Comparison of long-term vaccination titres, early vaccination titres and naturally acquired immunity to and booster effects on the measles virus. Vaccine 12, 129–133 (1994). [PubMed: 8147093]

24. Rosen JB, Rota JS, Hickman CJ, Sowers SB, Mercader S, Rota PA, Bellini WJ, Huang AJ, Doll MK, Zucker JR, Zimmerman CM, Outbreak of measles among persons with prior evidence of immunity, New York City, 2011. Clin. Infect. Dis 58, 1205–1210 (2014). [PubMed: 24585562]

25. Hahne SJ, Nic Lochlainn LM, van Burgel ND, Kerkhof J, Sane J, Yap KB, van Binnendijk RS, Measles outbreak among previously immunized healthcare workers, the Netherlands, 2014. J. Infect. Dis 214, 1980–1986 (2016). [PubMed: 27923955]

26. Bautista-López N, Ward BJ, Mills E, McCormick D, Martel N, Ratnam S, Development and durability of measles antigen-specific lymphoproliferative response after MMR vaccination. Vaccine 18, 1393–1401 (2000). [PubMed: 10618537]

27. Gans HA, Yasukawa LL, Sung P, Sullivan B, DeHovitz R, Audet S, Beeler J, Arvin AM, Measles humoral and cell-mediated immunity in children aged 5–10 years after primary measles immunization administered at 6 or 9 months of age. J. Infect. Dis 207, 574–582 (2013). [PubMed: 23300162]

28. Kontio M, Jokinen S, Paunio M, Peltola H, Davidkin I, Waning antibody levels and avidity: Implications for MMR vaccine-induced protection. J. Infect. Dis 206, 1542–1548 (2012). [PubMed: 22966129]

29. Naniche D, Garenne M, Rae C, Manchester M, Buchta R, Brodine SK, Oldstone MB, Decrease in measles virus-specific CD4 T cell memory in vaccinated subjects. J. Infect. Dis 190, 1387–1395 (2004). [PubMed: 15378430]

30. Mathias RG, Meekison WG, Arcand TA, Schechter MT, The role of secondary vaccine failures in measles outbreaks. Am. J. Public Health 79, 475–478 (1989). [PubMed: 2929807]

31. Anders JF, Jacobson RM, Poland GA, Jacobsen SJ, Wollan PC, Secondary failure rates of measles vaccines: A metaanalysis of published studies. Pediatr. Infect. Dis. J 15, 62–66 (1996). [PubMed: 8684879]

32. van Binnendijk RS, van der Heijden RW, Osterhaus AD, Monkeys in measles research. Curr. Top. Microbiol. Immunol 191, 135–148 (1995). [PubMed: 7789157]

33. McChesney MB, Miller CJ, Rota PA, Zhu YD, Antipa L, Lerche NW, Ahmed R, Bellini WJ, Experimental measles. I. Pathogenesis in the normal and the immunized host. Virology 233, 74–84 (1997). [PubMed: 9201218]

34. Lin WH, Kouyos RD, Adams RJ, Grenfell BT, Griffin DE, Prolonged persistence of measles virus RNA is characteristic of primary infection dynamics. Proc. Natl. Acad. Sci. U.S.A 109, 14989–14994 (2012). [PubMed: 22872860]

35. Auwaerter PG, Rota PA, Elkins WR, Adams RJ, DeLozier T, Shi Y, Bellini WJ, Murphy BR, Griffin DE, Measles virus infection in rhesus macaques: Altered immune responses and comparison of the virulence of six different virus strains. J. Infect. Dis 180, 950–958 (1999). [PubMed: 10479117]

36. Permar SR, Moss WJ, Ryon JJ, Monze M, Cutts F, Quinn TC, Griffin DE, Prolonged measles virus shedding in human immunodeficiency virus-infected children, detected by reverse transcriptase-polymerase chain reaction. J. Infect. Dis 183, 532–538 (2001). [PubMed: 11170977]

37. Riddell MA, Moss WJ, Hauer D, Monze M, Griffin DE, Slow clearance of measles virus RNA after acute infection. J. Clin. Virol 39, 312–317 (2007). [PubMed: 17625962]

38. Pitcher CJ, Hagen SI, Walker JM, Lum R, Mitchell BL, Maino VC, Axthelm MK, Picker LJ, Development and homeostasis of T cell memory in rhesus macaque. J. Immunol 168, 29–43 (2002). [PubMed: 11751943]

39. Ludlow M, Rennick LJ, Sarlang S, Skibinski G, McQuaid S, Moore T, de Swart RL, Duprex WP, Wild-type measles virus infection of primary epithelial cells occurs via the basolateral surface without syncytium formation or release of infectious virus. J. Gen. Virol 91, 971–979 (2010). [PubMed: 19923259]

40. Sinn PL, Williams G, Vongpunsawad S, Cattaneo R, McCray PB Jr., Measles virus preferentially transduces the basolateral surface of well-differentiated human airway epithelia. J. Virol 76, 2403–2409 (2002). [PubMed: 11836418]

41. de Swart RL, Yuksel S, Osterhaus AD, Relative contributions of measles virus hemagglutinin- and fusion protein-specific serum antibodies to virus neutralization. J. Virol 79, 11547–11551 (2005). [PubMed: 16103210]

42. Polack FP, Hoffman SJ, Crujeiras G, Griffin DE, A role for nonprotective complement-fixing antibodies with low avidity for measles virus in atypical measles. Nat. Med 9, 1209–1213 (2003). [PubMed: 12925847]

43. Halliley JL,Tipton CM, Liesveld J, Rosenberg AF, Darce J, Gregoretti IV, Popova L, Kaminiski D, Fucile CF, Albizua I, Kyu S, Chiang KY, Bradley KT, Burack R, Slifka M, Hammarlund E, Wu H, Zhao L, Walsh EE, Falsey AR, Randall TD, Cheung WC, Sanz I, Lee FE-H, Long-lived plasma cells are contained within the CD19⁻CD38^hiCD138⁺ subset in human bone marrow. Immunity 43, 132–145 (2015). [PubMed: 26187412]

44. Benner R, Hijmans W, Haaijman JJ, The bone marrow: The major source of serum immunoglobulins, but still a neglected site of antibody formation. Clin. Exp. Immunol 46, 1–8 (1981). [PubMed: 7039877]

45. Manz RA, Thiel A, Radbruch A, Lifetime of plasma cells in the bone marrow. Nature 388, 133–134 (1997). [PubMed: 9217150]

46. Elgueta R, de Vries VC, Noelle RJ, The immortality of humoral immunity. Immunol. Rev 236, 139–150 (2010). [PubMed: 20636814]

47. Esolen LM, Takahashi K, Johnson RT, Vaisberg A, Moench TR, Wesselingh SL, Griffin DE, Brain endothelial cell infection in children with acute fatal measles. J. Clin. Invest 96, 2478–2481 (1995). [PubMed: 7593637]

48. Allen IV, McQuaid S, Penalva R, Ludlow M, Duprex WP, Rima BK, Macrophages and dendritic cells are the predominant cells infected in measles in humans. mSphere 3, e00570–17 (2018). [PubMed: 29743202]

49. Ludlow M, Lemon K, de Vries RD, McQuaid S, Millar EL, van Amerongen G, Yuksel S, Verburgh RJ, Osterhaus AD, de Swart RL, Duprex WP, Measles virus infection of epithelial cells in the macaque upper respiratory tract is mediated by subepithelial immune cells. J. Virol 87, 4033–4042 (2013). [PubMed: 23365435]

50. Mesman AW, de Vries RD, McQuaid S, Duprex WP, de Swart RL, Geijtenbeek TB, A prominent role for DC-SIGN+ dendritic cells in initiation and dissemination of measles virus infection in non-human primates. PLOS ONE 7, e49573 (2012). [PubMed: 23227146]

51. Ludlow M, de Vries RD, Lemon K, McQuaid S, Millar E, van Amerongen G, Yuksel S, Verburgh RJ, Osterhaus AD, de Swart RL, Duprex WP, Infection of lymphoid tissues in the macaque upper respiratory tract contributes to the emergence of transmissible measles virus. J. Gen. Virol 94, 1933–1944 (2013). [PubMed: 23784446]

52. Rennick LJ, de Vries RD, Carsillo TJ, Lemon K, van Amerongen G, Ludlow M, Nguyen DT, Yuksel S, Verburgh RJ, Haddock P, McQuaid S, Duprex WP, de Swart RL, Live-attenuated measles virus vaccine targets dendritic cells and macrophages in muscle of nonhuman primates. J. Virol 89, 2192–2200 (2015). [PubMed: 25473055]

53. Sato H, Yoneda M, Honda T, Kai C, Morbillivirus receptors and tropism: Multiple pathways for infection. Front. Microbiol 3, 75 (2012). [PubMed: 22403577]

54. Yanagi Y, Takeda M, Ohno S, Measles virus: Cellular receptors, tropism and pathogenesis. J. Gen. Virol 87, 2767–2779 (2006). [PubMed: 16963735]

55. Dorig RE, Marcil A, Chopra A, Richardson CD, The human CD46 molecule is a receptor for measles virus (Edmonston strain). Cell 75, 295–305 (1993). [PubMed: 8402913]

56. Naniche D, Wild TF, Rabourdin-Combe C, Gerlier D, Measles virus haemagglutinin induces down-regulation of gp57/67, a molecule involved in virus binding. J. Gen. Virol 74, 1073–1079 (1993). [PubMed: 8509760]

57. Mühlebach MD, Mateo M, Sinn PL, Prufer S, Uhlig KM, Leonard VH, Navaratnarajah CK, Frenzke M, Wong XX, Sawatsky B, Ramachandran S, McCray PB Jr., Cichutek K, von Messling V, Lopez M, R. Cattaneo, Adherens junction protein nectin-4 is the epithelial receptor for measles virus. Nature 480, 530–533 (2011). [PubMed: 22048310]

58. Noyce RS, Bondre DG, Ha MN, Lin LT, Sisson G, Tsao MS, Richardson CD, Tumor cell marker PVRL4 (nectin 4) is an epithelial cell receptor for measles virus. PLOS Pathog. 7, e1002240 (2011).

59. Seki F, Someya K, Komase K, Takeda M, A chicken homologue of nectin-4 functions as a measles virus receptor. Vaccine 34, 7–12 (2016). [PubMed: 26549360]

60. Cannons JL, Tangye SG, Schwartzberg PL, SLAM family receptors and SAP adaptors in immunity. Annu. Rev. Immunol 29, 665–705 (2011). [PubMed: 21219180]

61. Detre C, Keszei M, Romero X, Tsokos GC, Terhorst C, SLAM family receptors and the SLAM-associated protein (SAP) modulate T cell functions. Semin. Immunopathol 32, 157–171 (2010). [PubMed: 20146065]

62. Tatsuo H, Ono N, Tanaka K, Yanagi Y, SLAM (CDw150) is a cellular receptor for measles virus. Nature 406, 893–897 (2000). [PubMed: 10972291]

63. de Swart RL, Ludlow M, de Witte L, Yanagi Y, van Amerongen G, McQuaid S, Yuksel S, Geijtenbeek TB, Duprex WP, Osterhaus AD, Predominant infection of CD150+ lymphocytes and dendritic cells during measles virus infection of macaques. PLOS Pathog. 3, e178 (2007). [PubMed: 18020706]

64. Leonard VH, Hodge G, Reyes-Del Valle J, McChesney MB, Cattaneo R, Measles virus selectively blind to signaling lymphocytic activation molecule (SLAM; CD150) is attenuated and induces

strong adaptive immune responses in rhesus monkeys. J. Virol 84, 3413–3420 (2010). [PubMed: 20071568]

65. Massé N, Ainouze M, Neel B, Wild TF, Buckland R, Langedijk JP, Measles virus (MV) hemagglutinin: Evidence that attachment sites for MV receptors SLAM and CD46 overlap on the globular head. J. Virol 78, 9051–9063 (2004). [PubMed: 15308701]

66. Navaratnarajah CK, Vongpunsawad S, Oezguen N, Stehle T, Braun W, Hashiguchi T, Maenaka K, Yanagi Y, Cattaneo R, Dynamic interaction of the measles virus hemagglutinin with its receptor signaling lymphocytic activation molecule (SLAM, CD150). J. Biol. Chem 283, 11763–11771 (2008). [PubMed: 18292085]

67. Erlenhöfer C, Duprex WP, Rima BK, ter Meulen V, Schneider-Schaulies J, Analysis of receptor (CD46, CD150) usage by measles virus. J. Gen. Virol 83, 1431–1436 (2002). [PubMed: 12029158]

68. Yanagi Y, Ono N, Tatsuo H, Hashimoto K, Minagawa H, Measles virus receptor SLAM (CD150). Virology 299, 155–161 (2002). [PubMed: 12202217]

69. Schneider U, von Messling V, Devaux P, Cattaneo R, Efficiency of measles virus entry and dissemination through different receptors. J. Virol 76, 7460–7467 (2002). [PubMed: 12097558]

70. Masse N, Barrett T, Muller CP, Wild TF, Buckland R, Identification of a second major site for CD46 binding in the hemagglutinin protein from a laboratory strain of measles virus (MV): Potential consequences for wild-type MV infection. J. Virol 76, 13034–13038 (2002). [PubMed: 12438629]

71. Vongpunsawad S, Oezgun N, Braun W, Cattaneo R, Selectively receptor-blind measles viruses: Identification of residues necessary for SLAM- or CD46-induced fusion and their localization on a new hemagglutinin structural model. J. Virol 78, 302–313 (2004). [PubMed: 14671112]

72. Santiago C, Bjorling E, Stehle T, Casasnovas JM, Distinct kinetics for binding of the CD46 and SLAM receptors to overlapping sites in the measles virus hemagglutinin protein. J. Biol. Chem 277, 32294–32301 (2002). [PubMed: 12065582]

73. Manchester M, Eto DS, Valsamakis A, Liton PB, Fernandez-Munoz R, Rota PA, Bellini WJ, Forthal DN, Oldstone MB, Clinical isolates of measles virus use CD46 as a cellular receptor. J. Virol 74, 3967–3974 (2000). [PubMed: 10756008]

74. Ono N, Tatsuo H, Hidaka Y, Aoki T, Minagawa H, Yanagi Y, Measles viruses on throat swabs from measles patients use signaling lymphocytic activation molecule (CDw150) but not CD46 as a cellular receptor. J. Virol 75, 4399–4401 (2001). [PubMed: 11287589]

75. Buckland R, Wild TF, Is CD46 the cellular receptor for measles virus? Virus Res. 48, 1–9 (1997). [PubMed: 9140188]

76. Shibahara K, Hotta H, Katayama Y, Homma M, Increased binding activity of measles virus to monkey red blood cells after long-term passage in Vero cell cultures. J. Gen. Virol 75, 3511–3516 (1994). [PubMed: 7996142]

77. Bartz R, Brinckmann U, Dunster LM, Rima B, Ter Meulen V, J. Schneider-Schaulies, Mapping amino acids of the measles virus hemagglutinin responsible for receptor (CD46) downregulation. Virology 224, 334–337 (1996). [PubMed: 8862431]

78. Bieback K, Lien E, Klagge IM, Avota E, Schneider-Schaulies J, Duprex WP, Wagner H, Kirschning CJ, Ter Meulen V, Schneider-Schaulies S, Hemagglutinin protein of wild-type measles virus activates toll-like receptor 2 signaling. J. Virol 76, 8729–8736 (2002). [PubMed: 12163593]

79. Takeuchi K, Nagata N, Kato SI, Ami Y, Suzaki Y, Suzuki T, Sato Y, Tsunetsugu-Yokota Y, Mori K, Van Nguyen N, Kimura H, Nagata K, Wild-type measles virus with the hemagglutinin protein of the Edmonston vaccine strain retains wild-type tropism in macaques. J. Virol 86, 3027–3037 (2012). [PubMed: 22238320]

80. Liljeroos L, Huiskonen JT, Ora A, Susi P, Butcher SJ, Electron cryotomography of measles virus reveals how matrix protein coats the ribonucleocapsid within intact virions. Proc. Natl. Acad. Sci. U.S.A 108, 18085–18090 (2011). [PubMed: 22025713]

81. Runkler N, Pohl C, Schneider-Schaulies S, Klenk HD, Maisner A, Measles virus nucleocapsid transport to the plasma membrane requires stable expression and surface accumulation of the viral matrix protein. Cell. Microbiol 9, 1203–1214 (2007). [PubMed: 17217427]

82. Salditt A, Koethe S, Pohl C, Harms H, Kolesnikova L, Becker S, Schneider-Schaulies S, Measles virus M protein-driven particle production does not involve the endosomal sorting complex required for transport (ESCRT) system. J. Gen. Virol 91, 1464–1472 (2010). [PubMed: 20130136]

83. Iwasaki M, Takeda M, Shirogane Y, Nakatsu Y, Nakamura T, Yanagi Y, The matrix protein of measles virus regulates viral RNA synthesis and assembly by interacting with the nucleocapsid protein. J. Virol 83, 10374–10383 (2009). [PubMed: 19656884]

84. Miyajima N, Takeda M, Tashiro M, Hashimoto K, Yanagi Y, Nagata K, Takeuchi K, Cell tropism of wild-type measles virus is affected by amino acid substitutions in the P, V and M proteins, or by a truncation in the C protein. J. Gen. Virol 85, 3001–3006 (2004). [PubMed: 15448363]

85. Tahara M, Takeda M, Yanagi Y, Contributions of matrix and large protein genes of the measles virus edmonston strain to growth in cultured cells as revealed by recombinant viruses. J. Virol 79, 15218–15225 (2005). [PubMed: 16306593]

86. Pohl C, Duprex WP, Krohne G, Rima BK, Schneider-Schaulies S, Measles virus M and F proteins associate with detergent-resistant membrane fractions and promote formation of virus-like particles. J. Gen. Virol 88, 1243–1250 (2007). [PubMed: 17374768]

87. Tahara M, Takeda M, Yanagi Y, Altered interaction of the matrix protein with the cytoplasmic tail of hemagglutinin modulates measles virus growth by affecting virus assembly and cell-cell fusion. J. Virol 81, 6827–6836 (2007). [PubMed: 17442724]

88. Abdullah H, Brankin B, Brady C, Cosby SL, Wild-type measles virus infection upregulates poliovirus receptor-related 4 and causes apoptosis in brain endothelial cells by induction of tumor necrosis factor-related apoptosis-inducing ligand. J. Neuropathol. Exp. Neurol 72, 681–696 (2013). [PubMed: 23771216]

89. Andres O, Obojes K, Kim KS, ter Meulen V, Schneider-Schaulies J, CD46- and CD150-independent endothelial cell infection with wild-type measles viruses. J. Gen. Virol 84, 1189–1197 (2003). [PubMed: 12692284]

90. Shivakoti R, Siwek M, Hauer D, Schultz KL, Griffin DE, Induction of dendritic cell production of type I and type III interferons by wild-type and vaccine strains of measles virus: Role of defective interfering RNAs. J. Virol 87, 7816–7827 (2013). [PubMed: 23678166]

91. Lemon K, de Vries RD, Mesman AW, McQuaid S, van G, Yuksel S, Ludlow M, Rennick LJ, Kuiken T, Rima BK, Geijtenbeek TB, Osterhaus AD, Duprex WP, de Swart RL, Early target cells of measles virus after aerosol infection of non-human primates. PLOS Pathog. 7, e1001263 (2011). [PubMed: 21304593]

92. de Vries RD, Lemon K, Ludlow M, McQuaid S, Yuksel S, van Amerongen G, Rennick LJ, Rima BK, Osterhaus AD, de Swart RL, Duprex WP, In vivo tropism of attenuated and pathogenic measles virus expressing green fluorescent protein in macaques. J. Virol 84, 4714–4724 (2010). [PubMed: 20181691]

93. van Binnendijk RS, van der Heijden RW, van Amerongen G, UytdeHaag FG, Osterhaus AD, Viral replication and development of specific immunity in macaques after infection with different measles virus strains. J. Infect. Dis 170, 443–448 (1994). [PubMed: 8035034]

94. Lin WH, Griffin DE, Rota PA, Papania M, Cape SP, Bennett D, Quinn B, Sievers RE, Shermer C, Powell K, Adams RJ, Godin S, Winston S, Successful respiratory immunization with dry powder live-attenuated measles virus vaccine in rhesus macaques. Proc. Natl. Acad. Sci. U.S.A 108, 2987–2992 (2011). [PubMed: 21282608]

95. Liesman RM, Buchholz UJ, Luongo CL, Yang L, Proia AD, DeVincenzo JP, Collins PL, Pickles RJ, RSV-encoded NS2 promotes epithelial cell shedding and distal airway obstruction. J. Clin. Invest 124, 2219–2233 (2014). [PubMed: 24713657]

96. Okamoto Y, Vricella LA, Moss WJ, Griffin DE, Immature CD4$^+$CD8$^+$ thymocytes are preferentially infected by measles virus in human thymic organ cultures. PLOS ONE 7, e45999 (2012). [PubMed: 23029357]

97. Condack C, Grivel JC, Devaux P, Margolis L, Cattaneo R, Measles virus vaccine attenuation: Suboptimal infection of lymphatic tissue and tropism alteration. J. Infect. Dis 196, 541–549 (2007). [PubMed: 17624839]

98. Grivel JC, Garcia M, Moss WJ, Margolis LB, Inhibition of HIV-1 replication in human lymphoid tissues ex vivo by measles virus. J. Infect. Dis 192, 71–78 (2005). [PubMed: 15942896]

99. Auwaerter PG, Kaneshima H, McCune JM, Wiegand G, Griffin DE, Measles virus infection of thymic epithelium in the SCID-hu mouse leads to thymocyte apoptosis. J. Virol 70, 3734–3740 (1996). [PubMed: 8648708]

100. Valsamakis A, Auwaerter PG, Rima BK, Kaneshima H, Griffin DE, Altered virulence of vaccine strains of measles virus after prolonged replication in human tissue. J. Virol 73, 8791–8797 (1999). [PubMed: 10482633]

101. Shivakoti R, Hauer D, Adams RJ, Lin WH, Duprex WP, de Swart RL, Griffin DE, Limited in vivo production of type I or type III interferon after infection of macaques with vaccine or wild-type strains of measles virus. J. Interf. Cytokine Res 35, 292–301 (2015).

102. Lin WW, Nelson AN, Ryon JJ, Moss WJ, Griffin DE, Plasma cytokines and chemokines in Zambian children with measles: Innate responses and association with HIV-1 coinfection and in-hospital mortality. J. Infect. Dis 215, 830–839 (2017). [PubMed: 28119485]

103. Zilliox MJ, Moss WJ, Griffin DE, Gene expression changes in peripheral blood mononuclear cells during measles virus infection. Clin. Vaccine Immunol 14, 918–923 (2007). [PubMed: 17538120]

104. Ovsyannikova IG, Reid KC, Jacobson RM, Oberg AL, Klee GG, Poland GA, Cytokine production patterns and antibody response to measles vaccine. Vaccine 21, 3946–3953 (2003). [PubMed: 12922130]

105. Pan CH, Greer CE, Hauer D, Legg HS, Lee EY, Bergen MJ, Lau B, Adams RJ, Polo JM, Griffin DE, A chimeric alphavirus replicon particle vaccine expressing the hemagglutinin and fusion proteins protects juvenile and infant rhesus macaques from measles. J. Virol 84, 3798–3807 (2010). [PubMed: 20130066]

106. Pan CH, Jimenez GS, Nair N, Wei Q, Adams RJ, Polack FP, Rolland A, Vilalta A, Griffin DE, Use of Vaxfectin adjuvant with DNA vaccine encoding the measles virus hemagglutinin and fusion proteins protects juvenile and infant rhesus macaques against measles virus. Clin. Vaccine Immunol 15, 1214–1221 (2008). [PubMed: 18524884]

107. Pan CH, Nair N, Adams RJ, Zink MC, Lee EY, Polack FP, Singh M, O'Hagan DT, Griffin DE, Dose-dependent protection against or exacerbation of disease by a polylactide glycolide microparticle-adsorbed, alphavirus-based measles virus DNA vaccine in rhesus macaques. Clin. Vaccine Immunol 15, 697–706 (2008). [PubMed: 18287579]

108. Pan CH, Valsamakis A, Colella T, Nair N, Adams RJ, Polack FP, Greer CE, Perri S, Polo JM, Griffin DE, Modulation of disease, T cell responses, and measles virus clearance in monkeys vaccinated with H-encoding alphavirus replicon particles. Proc. Natl. Acad. Sci. U.S.A 102, 11581–11588 (2005). [PubMed: 16037211]

109. Black FL, Sheridan SR, Studies on an attenuated measles virus vaccine IV. Administration of vaccine by several routes. N. Engl. J. Med 263, 165–169 (1960). [PubMed: 13801146]

110. Joyce JC, Carroll TD, Collins ML, Chen MH, Fritts L, Dutra JC, Rourke TL, Goodson JL, McChesney MB, Prausnitz MR, Rota PA, A microneedle patch for measles and rubella vaccination Is immunogenic and protective in infant rhesus macaques. J. Infect. Dis 218, 124–132 (2018). [PubMed: 29701813]

111. MVDP author group, Cape S, Chaudhari A, Vaidya V, Mulay R, Agarkhedkar S, Shermer C, Collins M, Anderson R, Agarkhedkar S, Kulkarni PS, Winston S, Sievers R, Dhere RM, Gunale B, Powell K, Rota PA, Papania M, Safety and immunogenicity of dry powder measles vaccine administered by inhalation: A randomized controlled Phase I clinical trial. Vaccine 32, 6791–6797 (2014). [PubMed: 25446830]

112. Griffin DE, Current progress in pulmonary delivery of measles vaccine. Expert Rev. Vaccines 13, 751–759 (2014). [PubMed: 24837839]

113. Low N, Bavdekar A, Jeyaseelan L, Hirve S, Ramanathan K, Andrews NJ, Shaikh N, Jadi RS, Rajagopal A, Brown KE, Brown D, Fink JB, John O, Scott P, Riveros-Balta AX, Greco M, Dhere R, Kulkarni PS, Henao Restrepo AM, A randomized, controlled trial of an aerosolized vaccine against measles. N. Engl. J. Med 372, 1519–1529 (2015). [PubMed: 25875257]

114. Low N, Kraemer S, Schneider M, Restrepo AM, Immunogenicity and safety of aerosolized measles vaccine: Systematic review and meta-analysis. Vaccine 26, 383–398 (2008). [PubMed: 18082295]

115. Beck SE, Laube BL, Barberena CI, Fischer AC, Adams RJ, Chesnut K, Flotte TR, Guggino WB, Deposition and expression of aerosolized rAAV vectors in the lungs of Rhesus macaques. Mol Ther. 6, 546–554 (2002). [PubMed: 12387250]

116. Kobune F, Sakata H, Sugiura A, Marmoset lymphoblastoid cells as a sensitive host for isolation of measles virus. J. Virol 64, 700–705 (1990). [PubMed: 2153236]

117. Ibricevic A, Pekosz A, Walter MJ, Newby C, Battaile JT, Brown EG, Holtzman MJ, Brody SL, Influenza virus receptor specificity and cell tropism in mouse and human airway epithelial cells. J. Virol 80, 7469–7480 (2006). [PubMed: 16840327]

118. Beauverger P, Buckland R, Wild F, Establishment and characterisation of murine cells constitutively expressing the fusion, nucleoprotein and matrix proteins of measles virus. J. Virol. Methods 44, 199–210 (1993). [PubMed: 8263115]
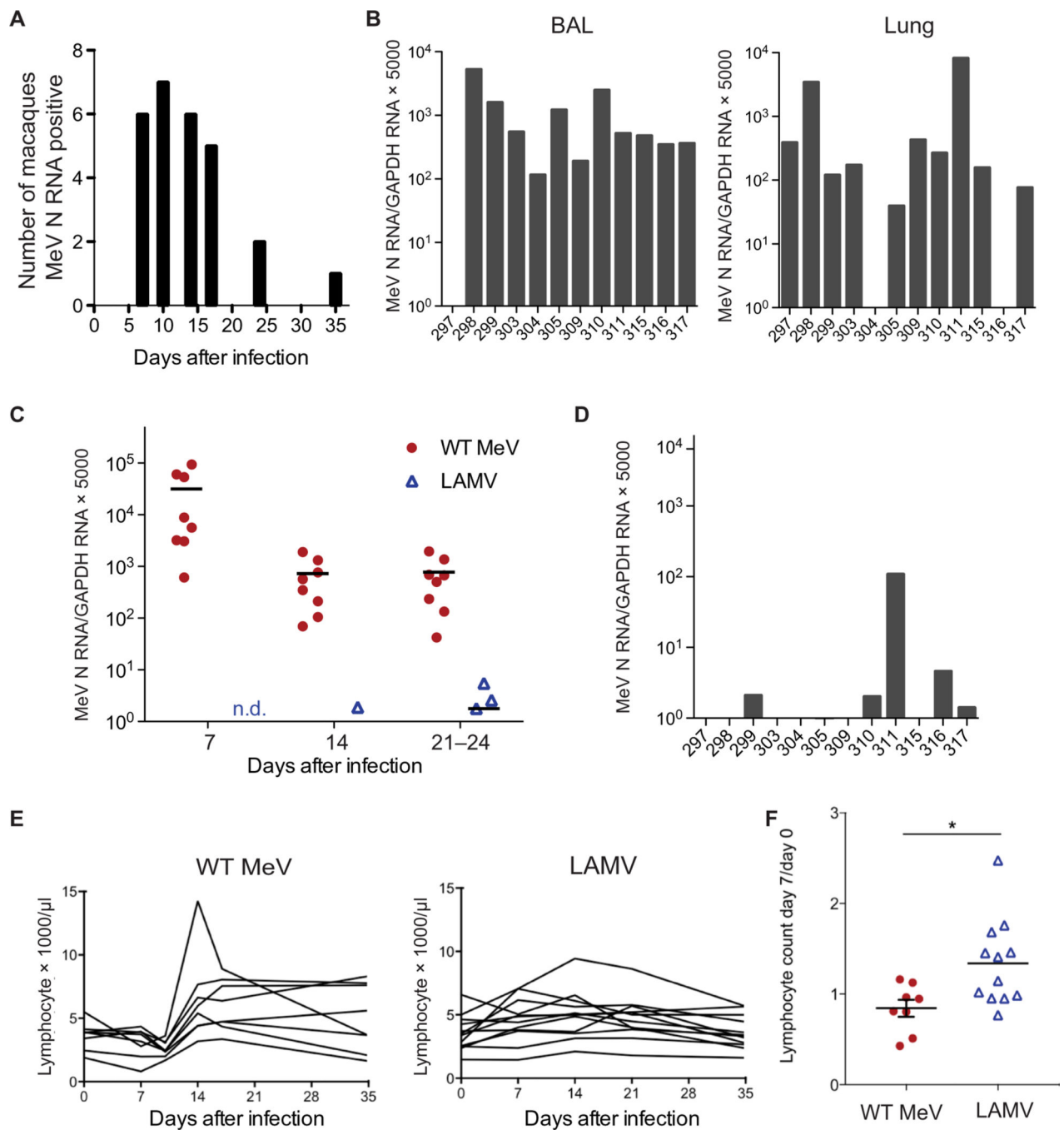
Fig. 1. Lymphocyte counts and MeV N RNA in the blood and respiratory tract of infected macaques.

MeV N–specific RT-PCR was used for detection and quantification of MeV N RNA after respiratory infection of macaques with either WT MeV or LAMV. (**A**) Number of macaques positive for MeV N RNA in nasal swab cell pellets from eight macaques 7 to 35 days after infection with WT MeV. (**B**) Quantification of MeV N RNA in bronchoalveolar lavage (BAL) fluids and lung tissues from 12 macaques 7 days after infection with LAMV. For quantification, MeV N RNA was normalized to the GAPDH control. Assays were performed

in duplicate, and averaged results are expressed as (number of copies of MeV N RNA)/ (number of copies of GAPDH RNA) $\times$ 5000. Numbers on the *x* axis identify individual macaques. (**C**) Comparison of the amounts of MeV N RNA in RNA extracted from 2×10^6 PBMCs from 12 LAMV-infected macaques or 8 WT MeV–infected macaques at 7, 14, 21, or 24 days after infection. *P* < 0.001. n.d., not detectable. (**D**) Quantification of MeV N RNA in the draining lymph nodes of 12 macaques 7 days after infection with LAMV. Numbers on the *x* axis identify individual macaques (**E**) Numbers of lymphocytes $\times$ 1000/μl of peripheral blood after infection of individual macaques with WT MeV or LAMV. (**F**) The ratio of day 7 to day 0 lymphocyte counts for macaques infected with WT MeV (red circles) or LAMV (blue triangles). Significance was determined by Student's *t* test, *P < 0.05.
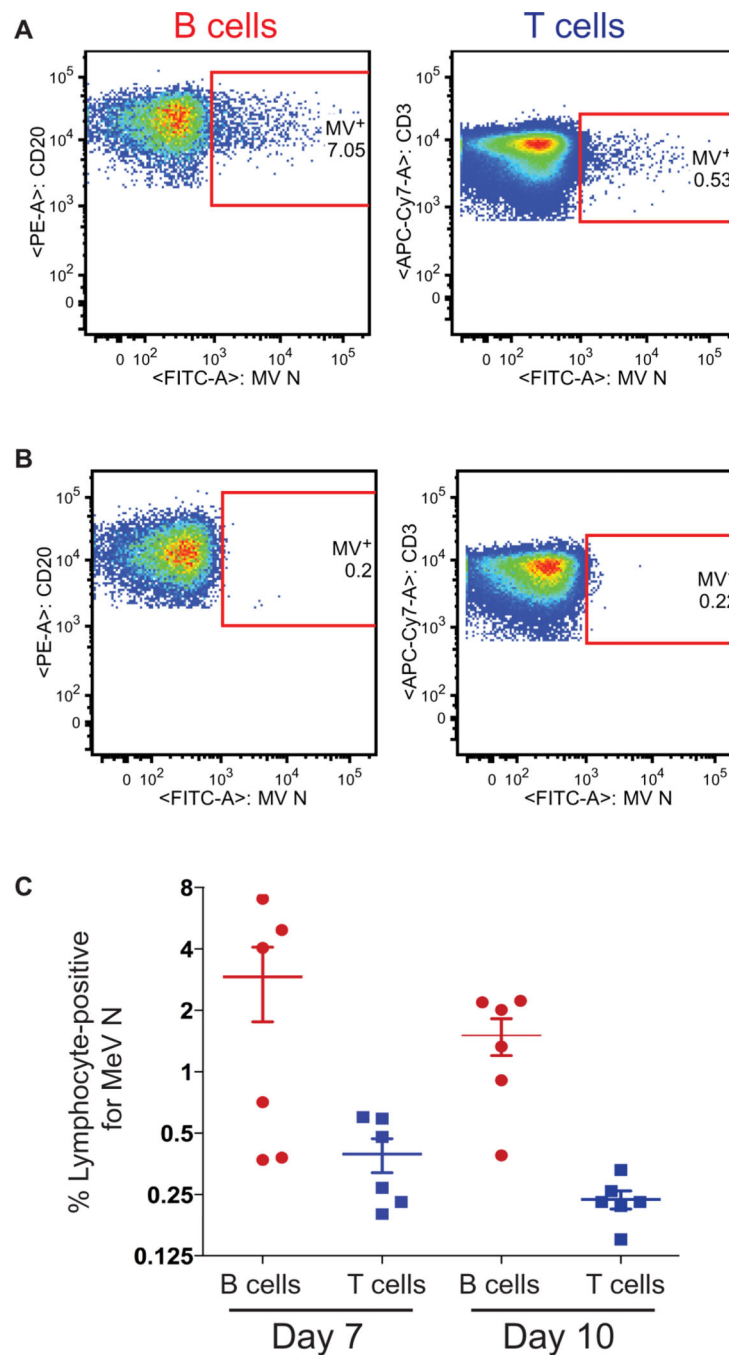
Fig. 2. Macaque PBMC subsets infected by WT MeV during viremia.
Flow cytometry was used to identify PBMCs expressing MeV N protein during viremia after intratracheal infection of macaques with 10^4 $TCID_{50}$ of WT MeV. Representative flow cytometry images are shown for MeV N protein–expressing CD20+ B cells and CD3+ T cells from WT MeV–infected macaques 7 days after infection (**A**) and from uninfected control macaques (**B**). PE, phycoerythrin; APC, allophycocyanin. (**C**) Per-centages of B cells (red circles) and T cells (blue squares) expressing MeV N protein 7 and 10 days after infection of macaques. Lines indicate the mean and SEM for each cell type and virus.
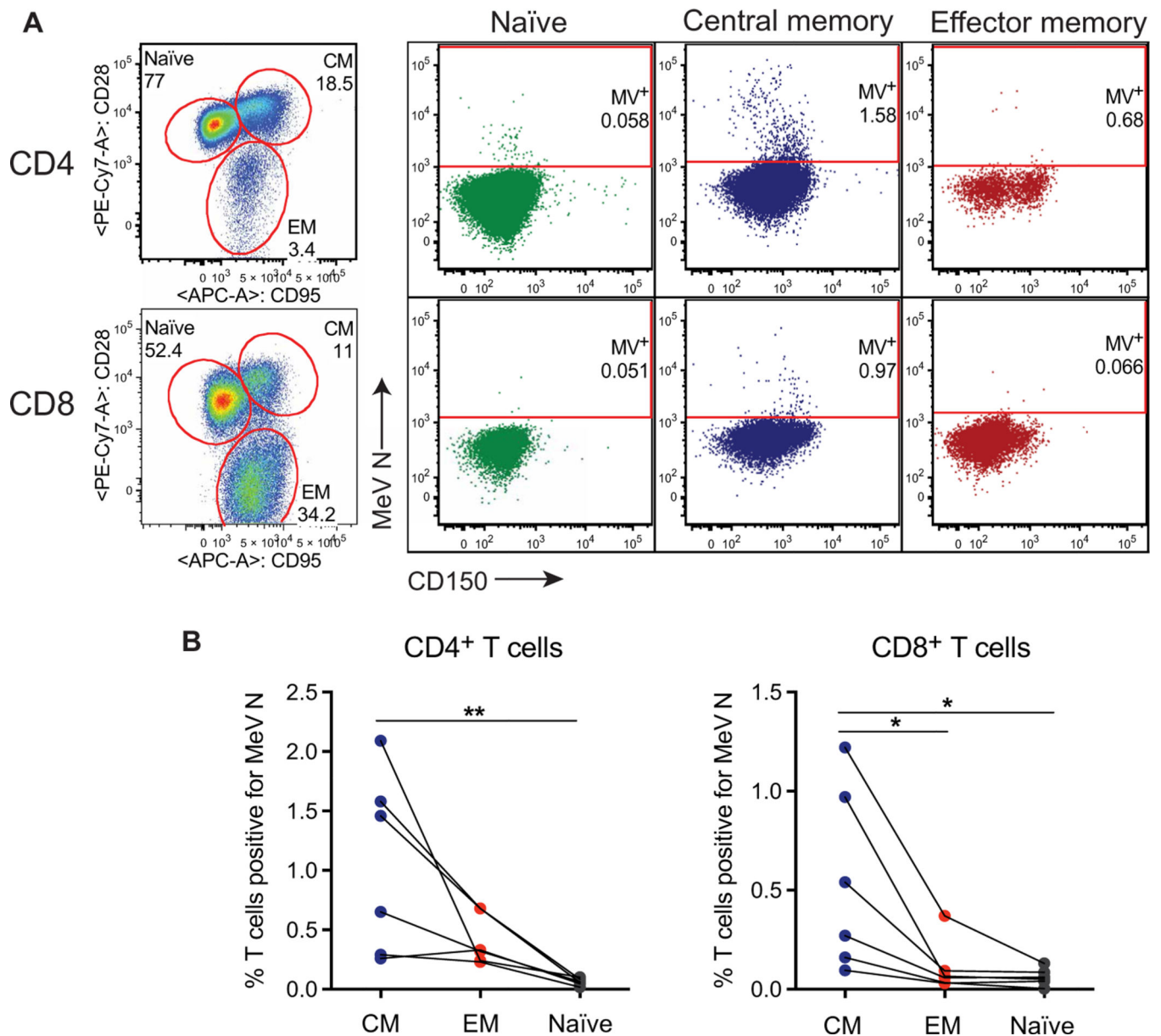
Fig. 3. Macaque T cell subsets infected by WT MeV during viremia.
(**A**) Representative flow cytometry images show MeV N protein–positive CD4+ T cells (top)
and CD8+ T cells (bottom) in the peripheral blood of macaques 7 days after infection with
10^4 TCID$_{50}$ of the Bilthoven strain of WT MeV. Gating (red) is shown for naïve T cells,
central memory (CM) T cells, and effector memory (EM) T cells (left), and MeV N protein–
positive T cells in each group (right). (**B**) Quantification of the percentages of MeV N
protein–positive CD4+ and CD8+ T cells that were central memory T cells, effector memory
T cells, and naïve T cells for six individual macaques. Results from the same macaque are
connected with lines. Significance was determined by ANOVA with Bonferroni post hoc
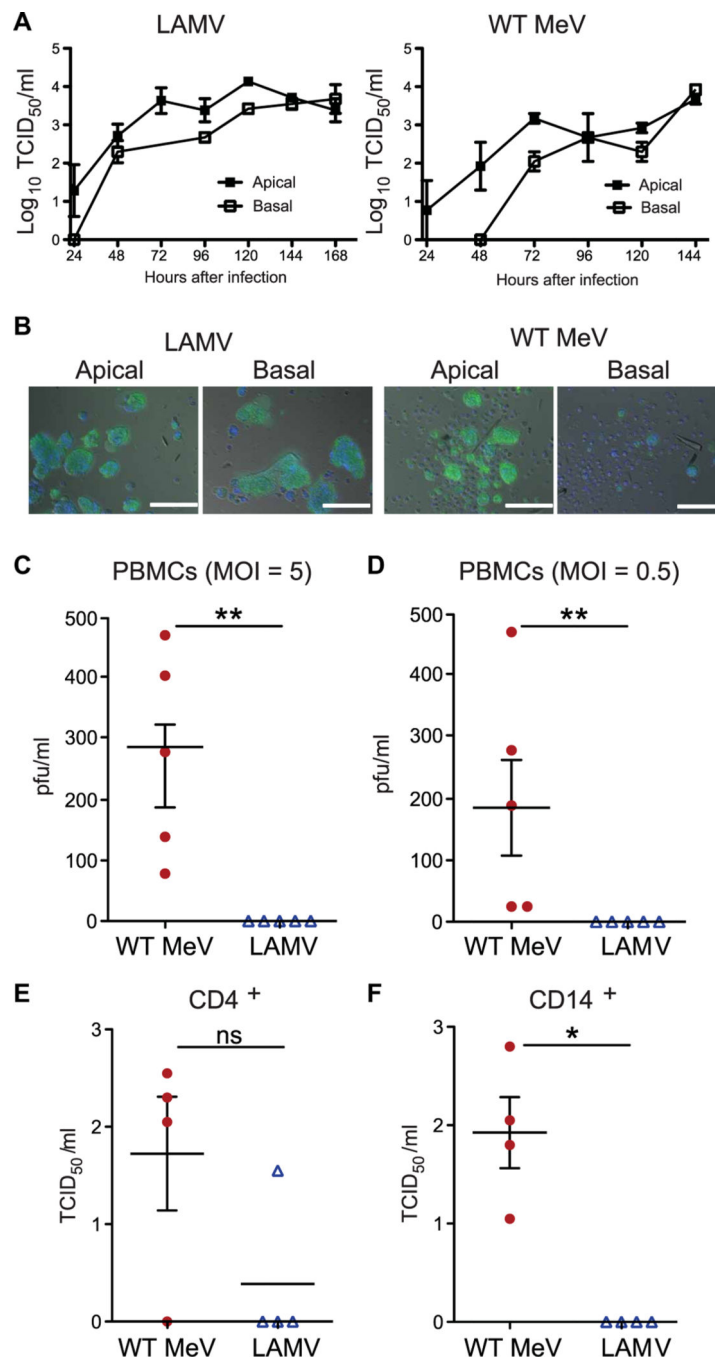tests. *$P < 0.05$, **$P < 0.01$.

Fig. 4. In vitro replication of WT MeV and LAMV in primary respiratory epithelial cells and PBMCs.

Infectious MeV in apical supernatants and shedding of MeV-infected multinuclear giant cells were measured after apical or basal infection of primary differentiated macaque tracheal epithelial cells with LAMV or WT MeV (MOI = 4.5). (**A**) Apical cell culture supernatants (cultures from three separate macaques; two replicates in each experiment) were assayed for infectious virus by a $TCID_{50}$ assay. Lines indicate the SEM. (**B**) Shed cells collected from macaque tracheal epithelial cell monolayers 144 hours after infection were

stained with antibody to MeV N protein and DAPI nuclear stain after fixation and permeabilization. Merged images of phase-contrast, MeV N protein expression (green), and DAPI nuclear stain (blue) are shown. Scale bar represents 150 μm. (**C** to **F**) Production of infectious virus 24 hours after infection of human PBMCs with WT MeV (red circles) and LAMV (blue triangles) at high (2 to 5) MOI (C) and low (0.5) MOI (D). Production of infectious virus 24 hours after infection of human CD4^{+} T cells (E) or CD14^{+} myeloid cells (F) with WT MeV (red circles) or LAMV (blue triangles) (MOI = 5). Horizontal line indicates the mean. Significance was determined by Mann-Whitney *U* test. *$P < 0.05$ and **$P < 0.01$. ns, not significant.
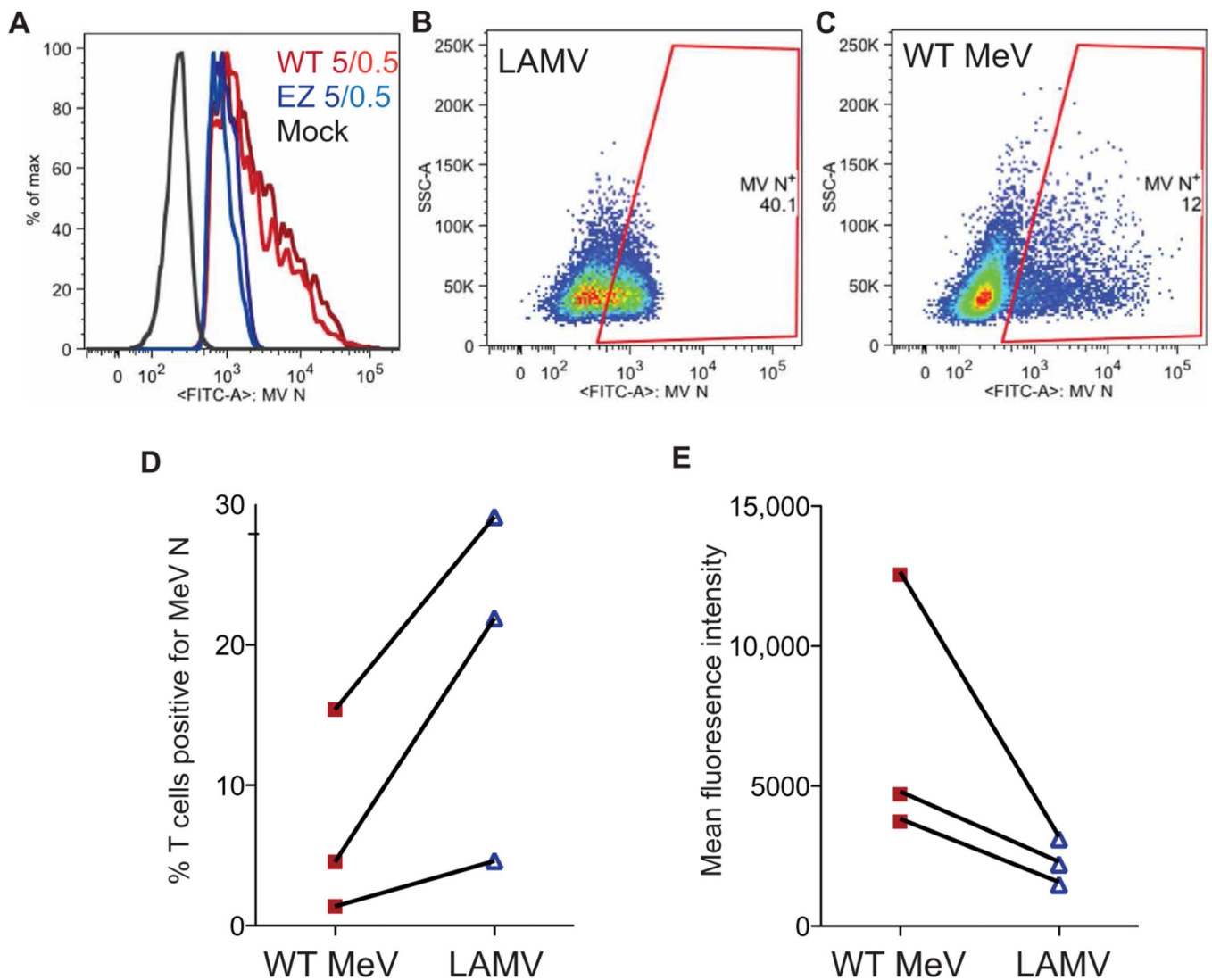
Fig. 5. In vitro replication of WT MeV and LAMV in human primary CD4+ T cells.
Shown is flow cytometry analysis of MeV N protein expression after in vitro infection of human PBMCs with WT MeV or LAMV (vaccine strain of MeV). (**A**) Flow cytometry histogram shows amounts of MeV N protein expressed by human CD4+ T cells 20 hours after infection with WT MeV or LAMV at an MOI of 0.5 or 5.0. (**B** and **C**) Flow cytometry plots of CD4+ T cell expression of MeV N protein 20 hours after infection with LAMV (B) or WT MeV (C) strains (MOI = 5.0). SSC, side-scattered light. (**D** and **E**) Each panel shows results of three separate flow cytometry experiments that assessed the percentage of human CD4+ T cells expressing MeV N protein (D) and the amount of MeV N protein measured by immunofluorescence (E) 48 hours after infection of human PBMCs with WT MeV or LAMV (MOI = 5). Lines connect data from the same experiment.
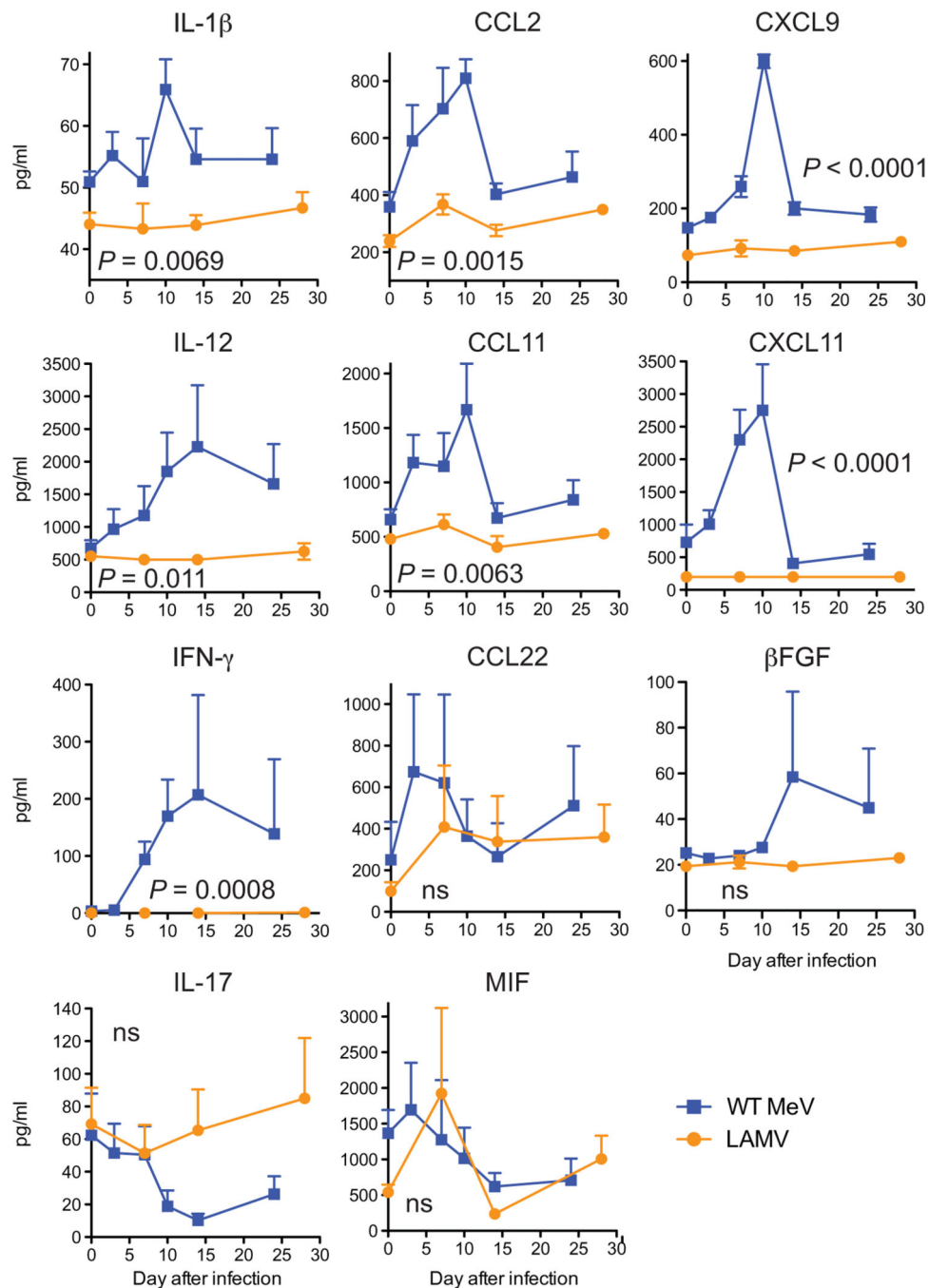
Fig. 6. Plasma cytokine and chemokine concentrations after WT MeV or LAMV infection of macaques.

Plasma concentrations of IL-1β, IFN-γ, IL-12, CCL2, CCL11, CCL22, CXCL9, CXCL11, MIF, and βFGF were measured using a Luminex 28-plex monkey cytokine/chemokine assay panel. Plasma samples were run in duplicate for five animals infected with WT MeV (blue) or with LAMV (orange). Data are plotted as means ± SEM. Significance of differences between groups was determined by two-way ANOVA using data from days 0, 7, 14, and 24 or 28 after infection. For analysis of IFN-γ, the two highest outliers (both in the WT MeV–infected group) were removed.
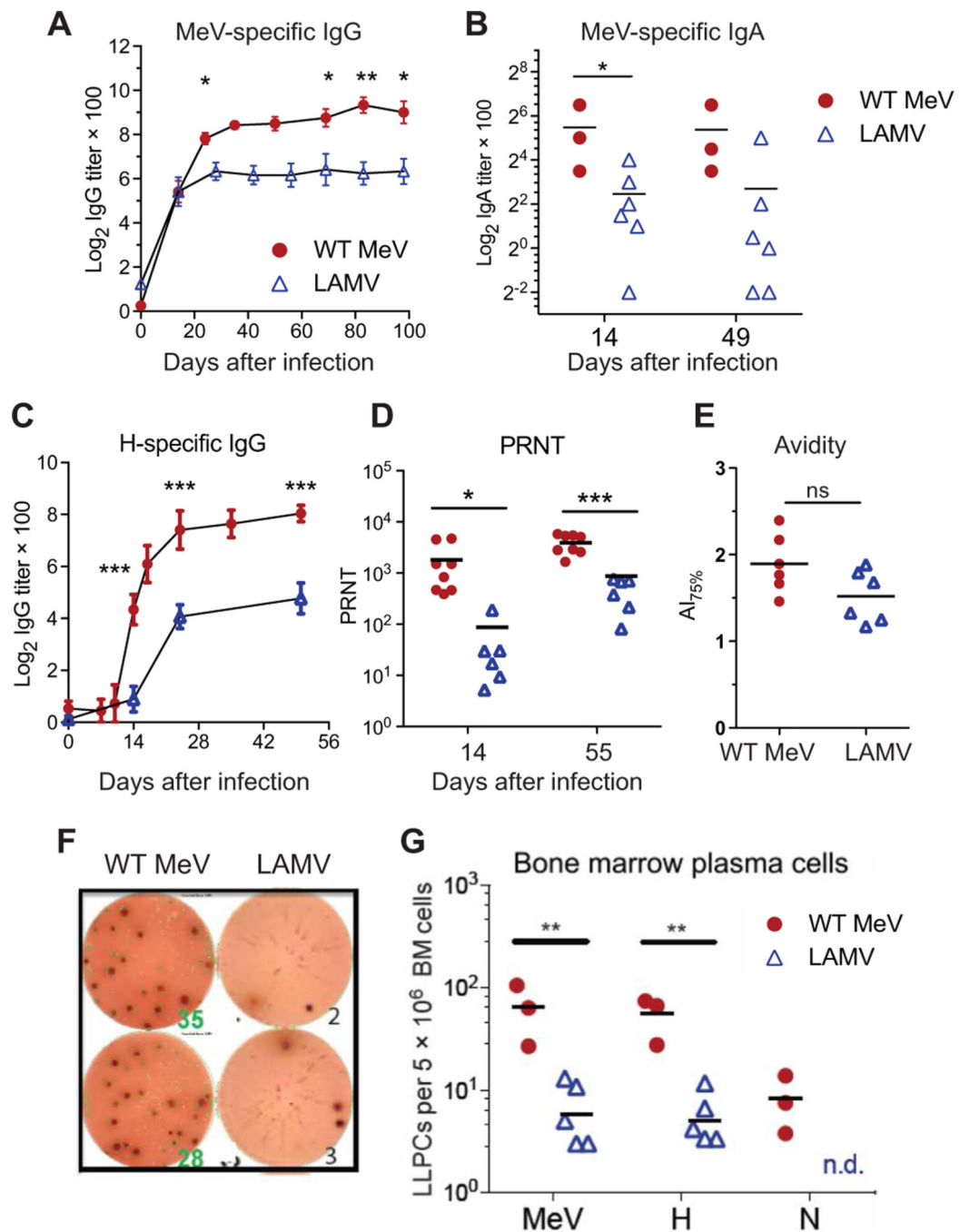
Fig. 7. MeV -specific antibody responses after WT MeV or LAMV infection of macaques.
Plasma concentrations of (**A**) MeV-specific IgG, (**B**) MeV-specific IgA, and (**C**) H-specific IgG were measured by enzyme immunoassay (EIA) using plates coated with a lysate from MeV-infected Vero cells or MeV H–expressing L cells. Titers of antibodies were determined on the basis of the curve of serially diluted plasma and assay-specific background values. (**D**) Reciprocal titers of neutralizing antibody in macaque plasma samples were determined by a plaque reduction neutralization test (PRNT) using the Chicago strain of MeV and Vero cells. Results were calculated from assay triplicates. (**E**) Avidity of MeV-specific IgG was

determined in triplicate by an EIA-based assay and expressed as avidity index (AI) for six individual macaques at 14 weeks after infection with WT MeV or LAMV. (**F**) MeV-specific IgG-secreting cells in the bone marrow were assessed by ELISpot assay to identify the numbers of cells secreting antibody to MeV. Shown are representative wells loaded with 5×10^5 bone marrow cells from macaques approximately one year after infection with WT MeV (35 and 28 spots) or LAMV (2 and 3 spots). Spots represent MeV-specific IgG-secreting long-lived plasma cells (LLPCs). (**G**) Number of MeV-, H-, and N-specific IgG-secreting long-lived plasma cells in macaque bone marrow assessed by ELISpot assay about 1 year after infection. Averaged number of spots from eight assay replicates in individual animals was plotted. *$P < 0.05$, **$P < 0.01$, and ***$P < 0.001$. Data in (A) and (B) were compared using two-way ANOVA with Bonferroni post hoc tests; data in (C), (D), (E), and (G) were compared using Student's *t* test.
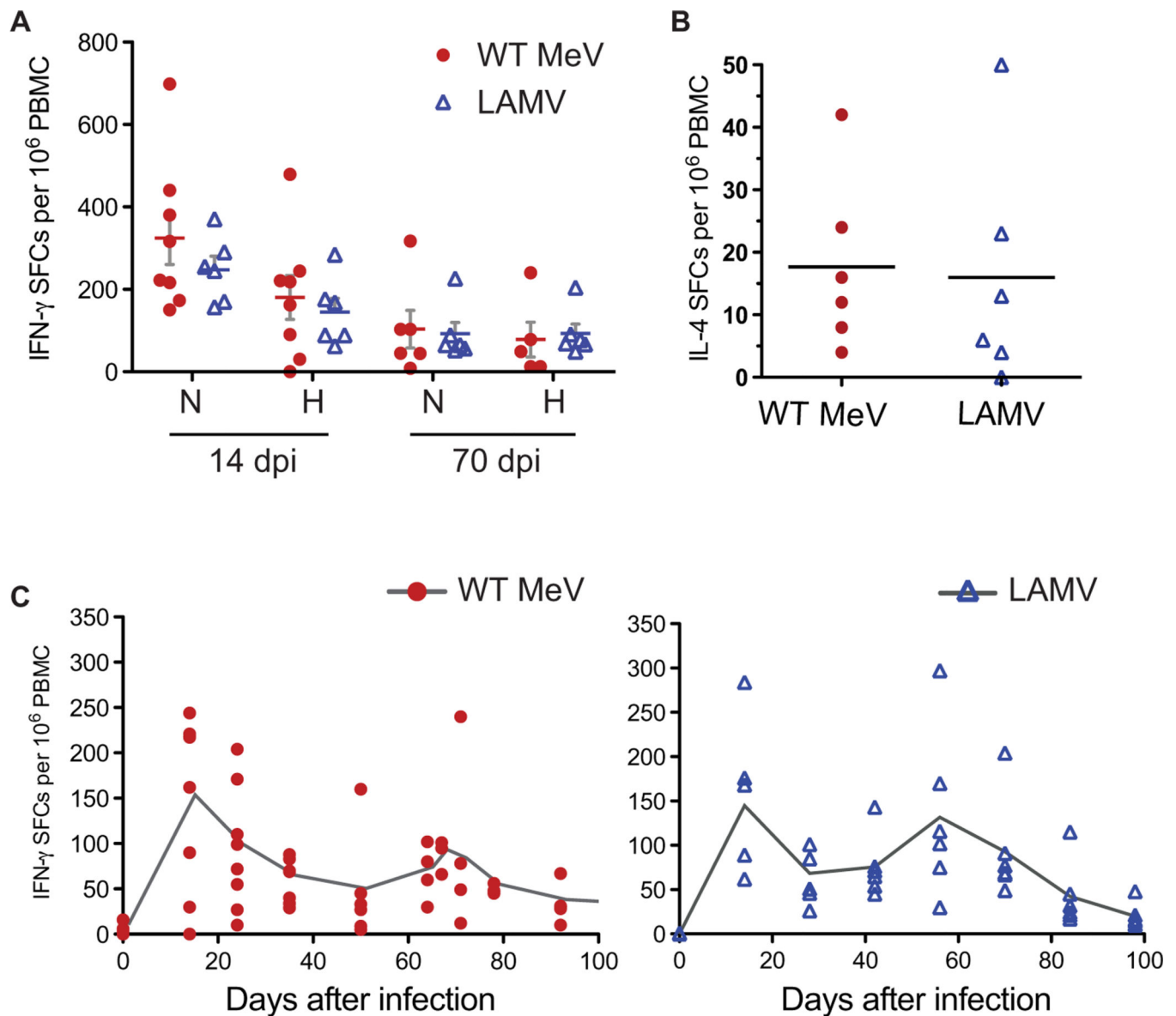
Fig. 8. Cellular immune responses after WT MeV and LAMV infection of macaques.
Numbers of IFN-γ– and IL-4–producing T cells in infected macaques were assessed by
ELISpot assay. Fresh macaque PBMCs (5×10^5) were added to multiscreen plates coated
with anti-human IFN-γ or IL-4 antibody in the presence of pooled H or N peptides or
medium. Data are reported as spot-forming cells (SFCs) after subtracting medium alone
wells from antigen-stimulated wells. (**A**) Numbers of H- and N-specific IFN-γ–producing
cells 14 and 70 days postinfection (dpi). (**B**) Numbers of N-specific IL-4–producing cells 14
days after infection. Horizontal line indicates the mean. (**C**) Changes in numbers of N-
specific IFN-γ–producing cells in the circulation of infected macaques over the course of
MeV infection. Reactivation of MeV-specific T cells in the circulation was noted around 60
days after infection for animals infected with WT MeV (red circles) or LAMV (blue
triangles).